On Some Low Temperature Hydrous Silicates Found in Japan.

By Tosio SUDO.

(Received May 10, 1943.)

CONTENTS.

Preface.

Although, nowadays, natural silicates are subjected to precise structural and chemical analyses resulting in a more complete classification, precise data are still almost lacking on some minerals, particularly, the low temperature hydrous silicates, which have the following characteristic physical and chemical properties:

(1) Since most of them are found as very minute crystals, intimately mixed with other substances, it is very difficult to secure large crystal flakes for making complete structural analyses and also to obtain pure specimens perfectly free from impurities in order to analyse them chemically.

(2) A large number of species are recognized owing to the wide substitution atom for atom in isomorphous silicates, affording interesting but difficult problems in the classification of these low temperature hydrous silicates.

(3) In the earlier days of mineralogy, most of the low temperature hydrous silicates were believed to be amorphous, but, recently, x-ray powder photographs have shown that almost all of them are crystalline clearly. It is also believed, however, that some of these minerals were originally in sol or gel condition, and gradually altered into the characteristic stable crystalline conditions in which we now see them, and a few of them are still in amorphous, whence it follows that studies of their occurrence or genesis must invoke the aid of colloid chemistry.

(4) These hydrous silicates occur as altered products of minerals that were formed at high temperature, and are also easily altered, these properties of which give rise to problems in geochemistry.

Having studied some of the Japanese low temperature hydrous silicates, the writer has summarized the results in this report.

The Chemical Compositions of Chamosite, Thuringite, and Aphrosiderite.

Introduction. Since chlorites usually occur either as aggregates of very fine crystal flakes or as powder intimately mixed with other substances, it is very difficult to measure their optical properties precisely or to obtain chemical analyses of pure crystals, and therefore the characteristic relations between their chemical compositions and their optical properties are still far from being fully established. A large number of species of chlorites within a limited range of composition are generally recognized. The above-mentioned properties of chlorites have made them the subject of investigation since the earliest days of mineralogy, resulting in various classifications by chemists as well as by mineralogists. In the past, classifications of chlorites, based mainly on their chemical compositions, have been attempted by R. F. Rammelsberg, G. Tschermak, W. J. Vernadsky, J. Jakob, A. N. Winchell, C. Doelter, C. Hintze, and J. Orcel. General introductions to these classifications have been published by C. Doelter[2], C. Hintze[1], and O. Orcel[3]. A. N. Winchell[4] first demonstrated the relations between their optical properties and their chemical compositions, showing the following mineral components.

Amesite (At) $H_4Mg_2Al_2SiO_9$, daphnite (Dn) $H_4Fe^{II}_2Al_2SiO_9$, cronstedite (Cr) $H_4Fe^{II}_2Fe_2SiO_9$, magnesio-cronstedite (MgCr) $H_4Mg_2Fe_2SiO_9$, kammererite (Kr) $H_4Mg_2Cr_2SiO_9$, antigorite (Ant) $H_4Mg_3Si_2O_9$, ferroantigorite (FeAnt) $H_4Fe_3Si_2O_9$, and nepouite (Np) $H_4Ni_3Si_2O_9$. J. Orcel[5] tried the classification of the chlorites by ratios as $s=SiO_2/R_2O_3$, $v=RO/R_2O_3$, $h=H_2O/R_2O_3$, $f=FeO/MgO$, $a=Fe_2O_3/Al_2O_3$. Recently, chemical formulae of the chlorites based on analyses of their crystal structure have been formulated. The formulae, shown by C. K. Swartz[6] are:

(a) Clinochlore family $R'_{13}(Al, Si_3)O_{10}(OH)_8$

$$R'_{13} = (Mg, Fe^{II}, Mn^{II})_5(Al, Fe^{III})$$

(b) Amesite family $R'_{14}(Al_2Si_2)O_{10}(OH)_8$

$$R'_{14} = (Mg, Fe^{II}, Mn^{II})_4(Al, Fe^{III})_2$$

According to H. Berman[7], the general formula of the chlorites is written

$$(Mg, Fe^{II})_{n-p}(Al, Fe^{III})_{2p}Si_{4-p}O_{10}(OH)_{2(n-2)}\,s\cdot H_2O$$

and an important characteristic of the chlorites is that Al and some Fe^{III} partly replace (Mg, Fe^{II}) and partly Si, whence the above formula may be written

$$[(Mg, Fe^{II})_{n-p}(Al, Fe^{III})_p][(Al, Fe^{III})_pSi_{4-p}]O_{10}(OH)_{2(n-2)}\cdot s\cdot H_2O$$

or $$(Mg, Fe^{II}, Al, Fe^{III})_n(Al, Fe^{III}, Si)_4O_{10}(OH)_{2(n-2)}\,sH_2O$$

According to H. Berman the chlorite family is divided into two main groups according to the number of n and p in the above formulae.

---

(1) C. Hintze, "Handbuch der Mineralogie," Bd. II, 678, Leipzig (1897).

(2) C. Doelter, "Handbuch der Mineralchemie," Bd. II, Zweiter Teil, 652, Leipzig (1917).

(3) J. Orcel, *Bull. soc. franç. minéral.*, **50**(1927), 75.

(4) A. N. Winchell, *Am. J. Sci.*, Fifth Series, **11**(1926), 283; *Am. Mieral.*, **13** (1928), 161; *Am. Mineral.*, **21**(1936), 642; A. N. Winchell, "Elements of Optical Mineralogy," 3rd Ed., Part II, 276, London (1927).

(5) J. Orcel, *Bull. soc. franç minéral.*, **50**(1927), 75.

(6) L. Pauling, *Proc. Nat. Acad. Sci.*, **16**(1930), 578; Ch. Mauguin, *Bull. soc. franç. minéral.*, **53**(1930), 279; R. C. McMurchy, *Z. Krist.*, **88**(1934), 420; C. K. Swartz, *Am. Mineral.*, **22**(1937), 1167.

(7) H. Berman, *Am. Mineral.*, **22**(1937), 378.

(1) The chlorite group (n=6)

(2) The leptochlorite group, (5.5>n>4, 2>p>0.7)

The leptochlorite group is divided roughly into two sections on the basis of differences in the n. According to H. Berman, the chlorites of the first section do not differ much from the chlorite group, but those of the second section show a definite departure from the chlorite group in the values of n, and in having higher p values, and much more F^{II} and Fe^{III} than the chlorite group.

Besides the precise classifications just mentioned, the chlorites are usually divided into three groups according to their chemical compositions, magnesium-rich, iron-rich, and their intermediate members.

The chlorites that are intimately associated with iron ores are usually iron-rich members, that is, iron chlorites, which are included in Berman's leptochlorite group. Of the large number of species included in iron chlorites, the compositions of some of them are doubtful and the definitely established members are as follows: chamosite, thuringite, aphrosiderite, daphnite, cronstedite, delessite, diabantite, strigovite, prochlorite, ripidolite, epichlorite, etc.

Chemical Compositions of Chamosite, Thuringite, and Aphrosiderite. The writer attempts, in this report, a graphical representation of the chemical compositions of three main species of iron chlorites, namely, chamosite, thuringite, and aphrosiderite. All of them are often detected in iron ores throughout the world. Fourteen analyses of chamosite, twenty-five of thuringite, and twenty of aphrosiderite, as collected by J. Orcel[10], H. Hintze[8], C. Doelter[9], and Dana[11], are used.

A horizontal line, on which the weight percentage of the mineral is represented by length from one end, is taken for each of the main components such as SiO_2, Al_2O_3, Fe_2O_3, FeO, MgO and H_2O, and numerous analytical results are plotted on it; the percentage of SiO_2 is plotted on the line for SiO_2, that of Al_2O_3 on the line for Al_2O_3, and so on. Of these plotted points, there are, on every line, many in one part and a little or none in others, showing the fluctuation of the chemical composition of the mineral. To show the fact more clearly the following treatment is adopted, which will be explained taking the case of SiO_2 of thuringite. Divide the line into parts of equal length, each corresponding to one per cent and named a unit. Count the plotted points contained in each unit and draw through the middle of every unit a vertical line upwards, representing the number of the point by length, connect the upper terminal points of the vertical lines by drawing a curve—the frequency curve of SiO_2. The same treatment is applied to all the other components and their frequency curves are also obtained. In Fig. 1 are shown the frequency curves of all the main components of three iron chlorites, thuringite, chamosite and aphrosiderite, and they show where these three minerals are chemically similar to or different from each other.

---

(8) C. Hintze, "Handbuch der Mineralogie," Bd. II, 736, 740, 748, Leipzig (1897).

(9) C. Doelter, "Handbuch der Mineralchemie," Bd. II, Dritter Teil, 324, 326, 335, Leipzig (1921).

(10) J. Orcel, *Bull. soc. franç minéral.*, **50**(1927), 75.

(11) E. S. Dana, "System of Mineralogy," Six Ed., 658, 657, 660, New York (1920).

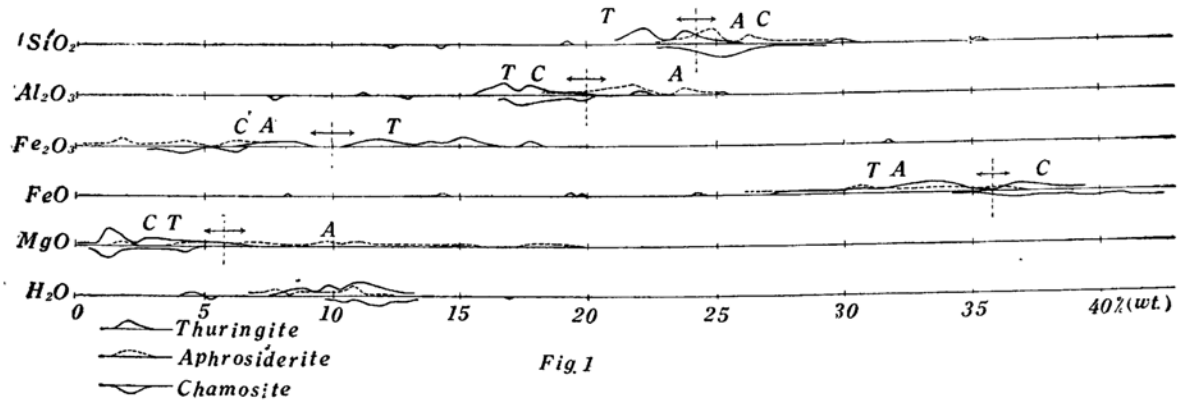

Fig. 1

The weight percentages of SiO_2, Al_2O_3, Fe_2O_3, etc. of chamosite, thuringite, and aphrosiderite are represented by the symbols $(SiO_2)_C$, $(SiO_2)_T$, $(SiO_2)_A$; $(Al_2O_3)_C$, $(Al_2O_3)_T$, $(Al_2O_3)_A$ etc. respectively, and the positions of the peaks of the frequency curves are indicated by suffix M, for example $(SiO_2)^M$, $(Al_2O_3)^M$, etc.

Then

(1) $21\% < (SiO_2)_T < 25\%$

$(SiO_2)_T^M \fallingdotseq 22^1/_4\%$ and $23^3/_4\%$

$(SiO_2)_C^M \fallingdotseq 25\%$

$24\% < (SiO_2)_A < 27\%$

$(SiO_2)_A^M \fallingdotseq 24^3/_4\%$ or $26^1/_4\%$

$(SiO_2)_T < (SiO_2)_A$, $(SiO_2)_T < (SiO_2)_C$

(2) $15\% < (Al_2O_3)_T < 19\%$, $(Al_2O_3)_T^M \fallingdotseq 16^1/_4\%$ or $17^3/_4\%$

$16\% < (Al_2O_3)_C < 20\%$, $(Al_2O_3)_C^M \fallingdotseq 17^1/_4\%$

$20\% < (Al_2O_3)_A < 25\%$, $(Al_2O_3)_A^M \fallingdotseq 21^3/_4\%$ or $23^3/_4\%$

$(Al_2O_3)_A > (Al_2O_3)_T$, $(Al_2O_3)_A > (Al_2O_3)_C$

(3) $10\% < (Fe_2O_3)_T < 18\%$, $(Fe_2O_3)_T^M \fallingdotseq 11^3/_4\%$, 15% or $17^3/_4\%$

$0\% < (Fe_2O_3)_A < 7\%$, $(Fe_2O_3)_A^M \fallingdotseq 1^3/_4\%$, 4%, $6^1/_4\%$

$3\% < (Fe_2O_3)_C < 7\%$, $(Fe_2O_3)_C^M \fallingdotseq 4^1/_4\%$, $6^1/_4\%$

$(Fe_2O_3)_T > (Fe_2O_3)_A$, $(Fe_2O_3)_T > (Fe_2O_3)_C$

(4) $27\% < (FeO)_T < 40\%$, $(FeO)_T^M \fallingdotseq 33^1/_4\%$, 37%

$26\% < (FeO)_A < 37\%$, $(FeO)_A^M \fallingdotseq 30^3/_4\%$

$35\% < (FeO)_C < 45\%$

$(FeO)_A < (FeO)_C$, $(FeO)_T < (FeO)_C$

(5) $0\% < (MgO)_T < 7\%$, $(MgO)_T^M \fallingdotseq 1^1/_4\%$

$0\% < (MgO)_C < 5\%$, $(MgO)_C^M \fallingdotseq 1^1/_4\%$, $4^1/_4\%$

$1\% < (MgO)_A < 20\%$, $(MgO)_A^M \fallingdotseq 10\%$

$(MgO)_A > (MgO)_T$, $(MgO)_A > (MgO)_C$

(6) $7\% < (H_2O)_T < 13\%$, $(H_2O)_T^M \fallingdotseq 11\%$
$6^1/_2\% < (H_2O)_A < 12\%$, $(H_2O)_A^M \fallingdotseq 10^3/_4\%$
$10\% < (H_2O)_C < 13\%$, $(H_2O)_C^M \fallingdotseq 11^1/_2\%$

From this representation of these chemical analyses, we find the following properties:

(a) By joining the plotted points of the weight percentages given by a chemical analysis, a vertically zig-zag line is obtained, as shown in Fig. 2, and such a zig-zag line has been obtained corresponding to each analysis of a mineral species. These zig-zag lines show a tendency to intersect almost at one point between every two horizontal lines (Fig. 2), and this must be because of replacements of some of SiO_2 by Al_2O_3, some Al_2O_3 by Fe_2O_3, some Fe_2O_3 by FeO (perhaps by oxidation), and some FeO by MgO.

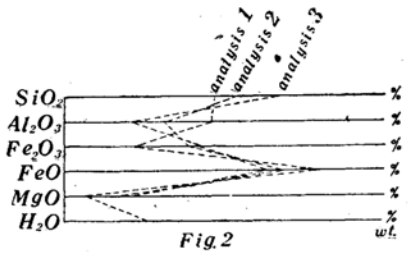

Fig. 2

(b) Generally the amount of H_2O (+) is almost constant not only in these three chlorites, but also in all the other chlorites. Following H_2O (+), the constancy in the weight percentages of Al_2O_3 was noticed.

(c) The degrees of frequency in the weight percentages of Al_2O_3, SiO_2, MgO, H_2O are found to be rather sharp, although the plotted points of the weight percentages of Fe_2O_3 and FeO are dispersed. This may be due to the restless property of the iron element, owing to the ease with which it is oxidized or leached. Generally speaking, the iron-rich silicates are easily altered by magmatic or underground waters, resulting in brown tarnishes. Although, in these alterations, we easily see oxidation or leaching of the iron element, the amounts of SiO_2, Al_2O_3, etc., remain almost unchanged, and because of this the ratio Fe_2O_3/FeO is never used to one of the standard numbers in discriminating the iron-rich silicates.

(d) In every frequency curve of SiO_2, Al_2O_3, MgO of thuringite and aphrodiderite, two peaks are always obtained, whereas in the curve of SiO_2, Fe_2O_3, Al_2O_3 of chamosite, we have only one.

Manganiferous Thuringite from Jōdoyama, near the Tateyama Hot Springs, Toyama Prefecture.

Introduction. The occurrence of a chlorite, ilmenite, garnet, etc. at Jōdoyama, near the Tateyama Hot Springs, Toyama Prefecture, has already been reported by Dr. D. Sato, who described the chemical composition of the chlorite without discussing the determination of the species(12). J. Orcel(13) added the analysis in his report as diabantite with the note "analyse incomplète". The writer examined the properties of this chlorite with the following results:

Occurrence. Jōdoyama mainly consists of hornblende diorite, showing a gneissic or partly mironitic structure. Vein-like bodies with sharp

(12) T. Wada, Beiträge zur Mineralogie von Japan, 296, Tokyo (1905–1915).
(13) J. Orcel, *Bull. soc. franç. minéral.*, **50**(1927), 75.

boundaries are found in the hornblende diorite, one of these being rich in hornblende and the other in chlorite, both being 2–3 m. wide at the saddle-shaped part between the two peaks, Jōdoyama and Oyama.

Microscopic Observations. The hornblende diorite, which consists mainly of hornblende, orthoclase, and plagioclase, with small amounts of epidote, is penetrated by small quartz veins. We find kaolinization in the feldspars, albitization in the plagioclase, and uralitization and chloritization in the hornblende. The hornblende, in parts, shows characteristic pleochroism as found in hastingsitic hornblende.

In masses rich in chlorite, such minerals as garnet, quartz, calcite, epidote, and hematite are observed as accessories. Often, a banded structure of the chlorite mass and the aggregate of crystal grains of garnet is met with. Frequently, the chlorite in very fine flakes is included in the quartz (Fig. 12), showing a vermicular appearance (Fig. 10. V). Garnet is included in the chlorite as anhedral grains, surrounded by quartz (Fig. 4) or calcite (Fig. 3) or both of them (Fig. 7). Garnet is included also in the quartz (Fig. 6) or calcite (Fig. 5 and 11) in the form of odd-looking ring-shaped fragments, often scattered about. The epidote is included in the chlorite mass as subhedral prismatic crystals. Small amounts of hematite are observed sporadically in the quartz (Figs. 6 and 8), or garnet (Fig. 11). Besides these, we meet with fragments of albitised plagioclase (Fig. 12) or fibrous skeleton crystals of hornblende (Fig. 13, H) which show a reddish tint by reflected light, and are also included in the quartz.

The mass rich in hornblende consists of hornblende mainly and small amounts of epidote (Fig. 14). The optical properties of the hornblende agree with those of hastingsite[14], namely,—refractive indices, $\alpha=1.720$, $\beta=1.723$, $\gamma=1.724$ (Na-light, at 28°C.); $2E \doteq 20°$; pleochroism, X..... green with yellowish-brown tint, Y $\doteq$ Z.... dark greenish-blue; absorption Z $\doteq$ Y>X. The maximum extinction angle along the prism zone is about 25°. The optic orientation may be Z=b, judging from the appearance of the cleavages. The epidote associated with the hastingsite is pleochroic, having a higher refractive index ($1.774<\gamma<1.778$) than that found in the hornblende diorite mass. The hornblende mass is penetrated by small albite veins in which hastingsite and small amounts of garnet and hematite are included.

Description of the Minerals. Epidote: Prismatic crystals, a few mm. long, were collected showing the following crystal forms: a(100), c(001), 1($20\bar{1}$), r($10\bar{1}$), s($20\bar{3}$), i($10\bar{2}$), ω(104), (105), n($\bar{1}11$), u(210), y(211). c(001) and n predominate, followed by a, u, and y.

Hematite: Micaceous hematite of a steel-black colour, metallic luster, and red streaks was found; the largest being 1 cm. in diameter. No reaction for titanium could be detected.

Garnet: Garnet is included mainly in the form of round altered grains about 0.5 mm. in mean diameter. In the fresh part, dodecahedron crystals of a reddish tint are rarely detected.

(14) M. P. Billings, *Am. Mineral.*, **13**(1928), 287.

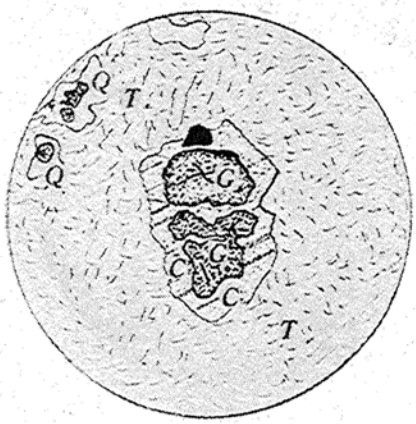

Fig. 3.

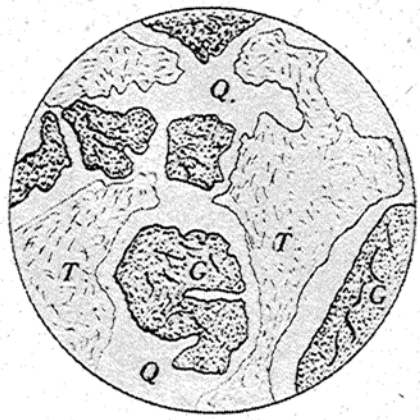

Fig. 4.

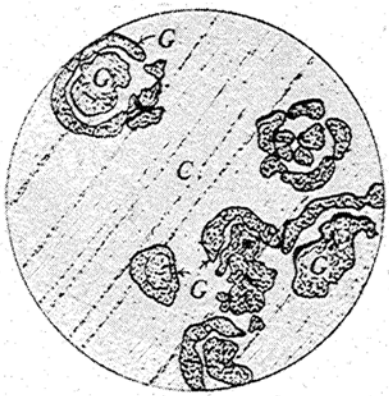

Fig. 5.

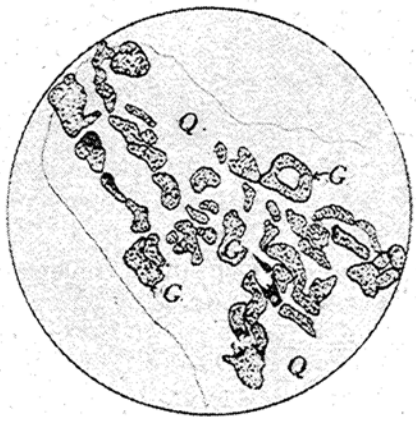

Fig. 6.

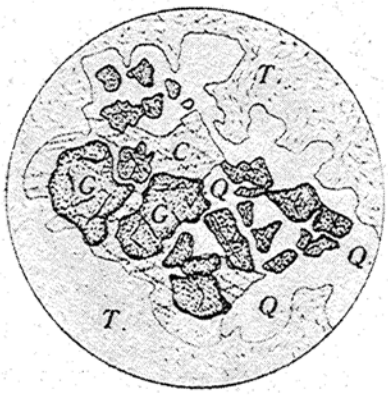

Fig. 7.

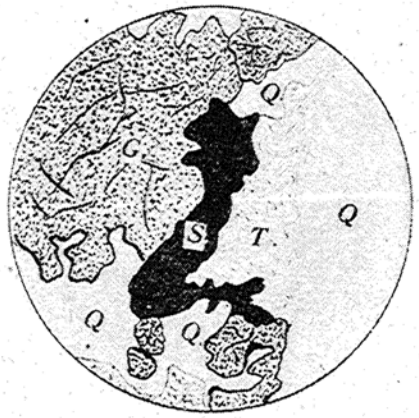

Fig. 8.

Fig. 3.—Fig. 8. (×50). Q: Quartz, G: Garnet, T: Chlorite (Manganiferous thuringite), C: Calcite, S: Hematite.

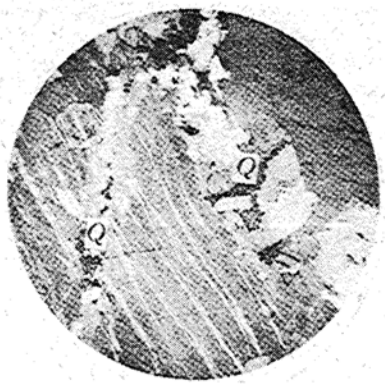

Fig 9.

Fig. 10.

Fig. 11.

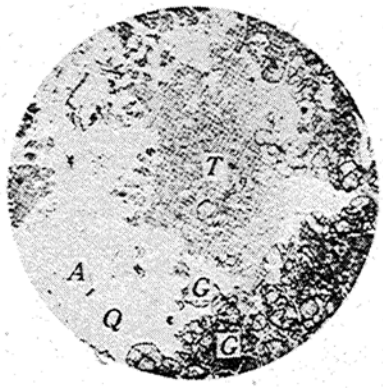

Fig. 12.

Fig. 13.

Fig. 14

Fig. 9.—Fig. 14. (×50). Q: Quartz, V: Chlorite included in quartz showing vermicular appearance, G: Garnet, S: Hematite, C: Calcite, T: Chlorite (Manganiferous thuringite), A: Albite, H: Hornblende (Hastingsite), E: Epidote.

Chlorite: The dark green mass that consists mainly of chlorite on being strongly heated in a blow-pipe flame, melts slightly to a black slaggish magnetic mass at the border. If the pulverized dark green mass is immersed in dilute hydrochloric acid and heated, the chlorite is easily decomposed, leaving colloidal silica behind. The optical constants of the chlorite are as follows: Refractive indices, α=1.623, β=1.628, γ=1.629, (Na-light, 20°C.); pleochroism, feeble; double refraction, low.

The aggregate was then broken up into small masses of chlorite and grains of garnet. The chlorite was separated from the garnet grains by means of a pincette, and analysed by the basic acetate method after fusing with alkali. The analysis is shown in Table 1, [1]. As seen from the analysis, the chlorite contains a fair amount of manganese, and the analysis almost agrees with that of thuringite with manganese replacing the ferrous iron. The chlorite is thus represented as manganiferous thuringite. J. Orcel showed the chlorite from Colorado in his report as "thuringite manganesifere", giving the analysis shown in Table 1, [2]. The analyses of the manganiferous thuringite of this locality and that of "thuringite manganesifere" shown by J. Orcel, are alike as shown in Table 1, [1] and [2].

The writer took the powder pattern of the chlorite compared it with that of thuringite from Saalfeld, Hartz, Germany, as described by A. H. Hallimond[15]. Clear agreement is noted as shown in Fig. 15, (1) and (2) and Table 2, [1] and [2]. No corrections were applied to the readings in Table 2, [1].

Table 1. Chemical Analyses of Manganiferous Thuringite.

	[1] Manganiferous thuringite (Jōdoyama, the Tateyama hot springs, Toyama Prefecture, Japan)	[2] "Thuringite manganesifere"[16] (Colorado)
SiO_2	22.24	24.34
Al_2O_3	17.05	16.46
Fe_2O_3	13.38	12.04
FeO	26.26	28.89
MnO	5.42	2.75
CaO	tr.	—
MgO	4.10	5.41
$H_2O(+)$	10.05	9.19
$H_2O(-)$	0.98	0.35
Total	99.48	99.80

(15) A. F. Hallimond, *Mineralog., Mag.*, **25**(1939), 445.

(16) J. Orcel, *Bull. soc. franç. minéral.*, **50**(1927), 75.

Table 2. X-ray Powder Photographs of Thuringite.

[1]			[2]	
I	$2l$ (cm.)	d (A.)	I	d (A.)
10	1.55	6.63	s	6.80
3	2.27	4.54	w	4.62
8	3.01	3.44	s	3.48
3	3.77	2.77	w	2.78
			vvw	2.65
3	4.09	2.56	m	2.59
			m	2.54
3	4.30	2.44	mw	2.45
3	4.42	2.38	mw	2.42
3	4.67	2.26	mw	2.25
7	5.32	2.00	m	2.00
3	5.67	1.88	w	1.88
			vvw	1.81
			vvw	1.76
			vvw	1.66
8	7.00	1.56	ms	1.55
4	7.20	1.52	w	1.51
3	7.96	1.40	vvw	1.42
4	8.00	1.39	w	1.39
			w	1.33
			vw	1.30

I: Intensity; d: Measured Spacing; $2l$: Distance between two corresponding powder lines measured on the film. [1] Manganiferous thuringite (Jōdoyama, the Tateyama hot springs, Toyama Prefecture, Japan.). Unfiltered Co radiation. Camera radius 28.65 mm. [2] Thuringite (Saalfeld, Harz, Germany). After A. F. Hallimond, *Mineralog. Mag.*, **25**(1939), 445.

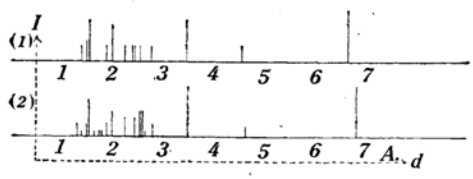

Fig. 15.

(1) Manganiferous thuringite (Jōdoyama, Japan).
Unfiltered Co radiation. Camaera radius, 28.65 mm.
(2) Thuringite (Saalfeld, Harz, Germany). After A. F. Hallimond: *Mineralog. Mag.*, **25** (1939), 445.
The lengths of lines in this diagram show roughly the relative intensities of the reflections. (I: Intensity, d: Spacing.)

Chamosite from the Arakawa Mine, Akita Prefecture.

Introduction. Although the chlorites usually occur as minute crystal flakes intimately mixed with other substances (clayey matter, siderite, etc.) in iron ores, in coal measures etc., they are found also in quartz veins etc. as pure aggregates of relatively large crystal flakes. The latter occurrence of the chlorite is chiefly observed in Japan proper.

Occurrence[17]. The occurrence has already been noticed of a chlorite that occurs as dark green spherical or cylindrical aggregates (Fig. 16) in quartz veins with prisms of quartz up to 3 cm. in length and in irregular masses of chalcopyrite from the Arakawa mine, Akita Prefecture, Japan.

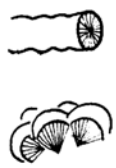

Fig. 16.

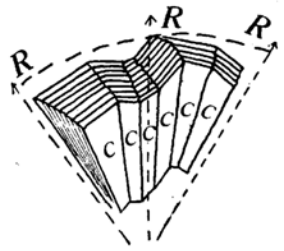

Fig. 17.

C : Cleavage faces.
R : Directions of radial axes.

The cylindrical-shaped aggregate consists of several spherical aggregations arranged in almost a straight line. These aggregates are either radially arranged groups or fan-shaped groups of crystals, tabular on their cleavage faces (Fig. 17). The lamellae are soft and flexible.

Microscopic Observations. Under the microscope, fan-like tufts with radial extinction are observed, including quartz grains or small patches of chalcopyrite. The optical constants of the chlorite—almost uniaxial negative; refractive indices, $\alpha=1.643$ $\beta \fallingdotseq \gamma=1.655$ (12.5°C.); pleochroism, $Z \fallingdotseq Y$.... green, X.... pale yellow to pale greenish-yellow; absorption, $X<Z \fallingdotseq Y$. X is almost normal to the cleavage faces. No one has yet reported the detailed and precise optical constants of chamosite.

Chemical Analysis[18]. These aggregates of the chlorite were broken up and reduced to a lath-shaped flaky powder, from which the chlorite alone was separated by means of a pincette, and analysed by the usual method. The chlorite was also readily decomposed by hot dilute hydrochloric acid leaving colloidal silica behind[19]. The analysis and the molecular proportion agree with the earlier analyses of chamosite, especially that described by A. F. Hallimond[20].

---

(17) About the general occurrence of chamosite: T. Deans, *Geol. Mag. London*, **71**(1934), 49; V. A. Eyles, *Mem. Geol. Survey, Scotland*, (1930), 67; G. V. Wilson, *Mem. Geol. Survey, Scotland*, (1930), 209; A. F. Hallimond, *Mineralog. Mag.*, **25** (1939), 443.

(18) About Chemical analyses of chamosite: C. Doelter, "Handbuch der Minerachemie," Bd. II, Dritter Teil, 324, Leipzig (1921); C. Hintze, "Handbuch der Mineralogie," Bd. II, 736, Leipzig (1897); E. R. Zalinski, *Neues Jahrb. Mineral. Geol.*, Beilage Band, A, **19**(1904), 40; H. Jung, *Chem. Erde*, **6**(1931), 275; A. F. Hallimond, *Mineralog. Mag.*, **25**(1929), 445; J. Orcel, *Bull. soc. franç. minéral.*, **50**(1927), 75; H. Berman, *Am. Mineral.*, **22**(1937), 381.

(19) About acid extraction: T. Deans, *Geol. Mag. London*, **71**(1934), 49.

(20) A. F. Hallimond, *Mineralog. Mag.*, **25**(1939), 446.

Table 3. Earlier Analyses of Chamosite.

	[1]	[2]	[3]	[4]	[5]	[6]	[7]	[8]	[9]	[10]	[11]	[12]
SiO_2	22.81	25.23	23.54	23.39	25.17	25.21	27.29	19.77	24.9	26.65	25.04	24.50
Al_2O_3	18.06	19.97	18.15	18.64	19.40	20.08	17.13	12.40	15.6	16.14	20.10	16.32
Fe_2O_3	2.58	—	3.67	6.06	—	—	4.06	5.74	7.2	6.69	2.05	7.45
FeO	36.55	37.51	36.84	34.34	41.60	41.31	39.42	31.02	35.0	34.43	35.40	31.46
MnO	—	—	—	—	—	—	—	0.35	0.4	—	—	3.33
CaO	1.49	—	1.62	1.55	—	—	—	3.34	—	—	—	—
MgO	4.28	4.39	1.35	1.44	1.45	1.53	—	3.63	4.6	4.47	4.28	4.59
Na_2O	—	—	—	—	—	—	—	—	—	—	—	—
K_2O	—	—	—	—	—	—	—	—	—	—	—	—
$H_2O(-)$	—	—	—	—	—	—	—	—	—	0.08		—
$H_2O(+)$	11.67	12.90	11.58	11.01	12.38	11.87	13.10	—	12.3	11.42	12.87	11.36
Total	(99.31)	100.00	(96.75)	(96.43)	100.00	100.00	100.00	(88.85)	100.0	99.88	99.74	99.01

[1] Windgälle (Uri), C. Schmidt, *Z. Krist.*, **11**(1886), 600. (TiO_2 1.11, CO_2 0.76).
[2] The analysis gives (1), after deducting carbonates, etc. and recalculating to 100%.
[3] Schmiedefeld, Thuringia, E. R. Zalinski, *Neues. Jarhb. Mineral. Geol.*, Beilage Band, **19**(1904), 46.
[4] Same as [3].
[5] The analysis of [3], after deducting CaO, FeO, and recalculating to 100%.
[6] The analysis of [4], after deducting CaO, FeO, and recalculating to 100%.
[7] Schmiedefeld, Thuringia, Loretz, *Z. Krist.*, **13**(1887), 52.
[8] Frodingham, Lincolnshire, A. F. Hallimond, *Mineralog. Mag.*, **25**(1939), 445.
[9] The Frodingham analysis, after deducting the carbonates, etc., and recalculating to 100%.
[10] Schmiedefeld, Thuringia, H. Jung, *Chem. Erde*, **6**(1931), 275.
[11] Hayanges, Lorraine, N. S. Kurnakov, V. V. Chernykih, *Mem. soc. russe. minéral.*, ser. 2, **55**(1926), 183–194.
[12] Chamosite from the Arakawa mine, Akita Prefecture.

The formula of the chamosite from this locality is represented as 2.9 (Fe^{II}, Mn, Mg)·1.0 (Al, Fe^{III})·2.0 SiO_2·aq. and agrees perfectly with Hallimond's formula[21] of 3 $RO{\cdot}R_2O_3{\cdot}2SiO_2$·aq. An important characteristic in this case is that manganese replaces a part of the ferrous iron, that is, the chlorite is given as manganiferous chamosite. The earlier chemical analyses and formulae of chamosite are shown in Tables 3 and 4 respectively.

Table 4. Chemical Formulae of Chamosite.

Tschermak	$Sp_4At_3At_3'$
E. R. Zalinski	$H_6(Fe^{II}, Mg)_3Al_2Si_2O_{13}$
H. Jung	$5Al_2O_3{\cdot}15(Fe^{II}, Mg)O{\cdot}11SiO_2{\cdot}16H_2O$
H. Berman	$n = 5.5,\ p = 1.2,\ Mg/Fe^{II} = 0.09$
A. F. Hallimond	$3RO{\cdot}R_2O_3{\cdot}2SiO_2$·aq.

(21) A. F. Hallimond, *Mineralog. Mag.*, **25**(1939), 446.

X-ray Powder Photographs[22] (Fig. 18, (3)). H. Jung[23] found that the powder photographs of chamosite and thuringite differ from each other. Later Hallimond[24] noticed that powder photographs of most of

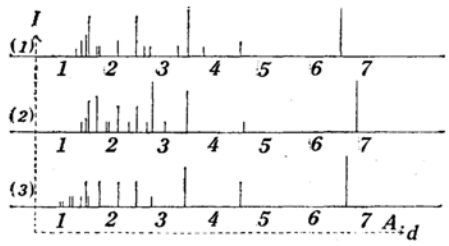

Fig. 18.

(1) Chamosite (Dairissikō, Rinkō Prefecture, Tūka Province, Manchoukuo). Unfiltered Fe radiation. Camera radius 30.28 mm.
(2) Chamosite (Dairissikō, Rinkō Prefecture, Tūka Province, Manchoukuo). Unfiltered Fe Radiation. Camera radius 28.65 mm. Presented by Mr. Sakurai.
(3) Chamosite (The Arakawa mine, Japan). Unfiltered Co radiation. Camera radius 28.65 mm.

The length of lines in this diagram show roughly the relative intensities of the reflections. (I: Intensity, d: Spacing.)

the chlorites belong to a type called the normal chlorite type, whereas those of the three species, chamosite, amesite, and cronstedite differ from each other and also from the normal chlorite type.

Generally speaking, in powder photographs of chlorites, we see chiefly three powder lines A, B, C, (d_A=7.04–6.72 A., d_B=4.68–4.49 A., d_C=3.53–3.41 A.) and a group of powder lines (d=1–3 A.). Certain differences are always noticed in every powder photograph of chlorites of different species and even of the same species, for example, the lack or presence of some weak powder lines or certain differences in the intensities and measured spacings of the powder lines. In a general investigation of powder photographs of all the chlorites, in most cases, the A and C lines are very strong, while the intensity of the B line is variable (even in patterns of the same species) and the measured spacings represented from these three lines are not constant. The differences in these measured spacings are as follows: d_A=7.04–6.72 A., d_B=4.68–4.49 A., d_C=3.53–3.41 A. (after A.F. Hallimond). Some differences are also seen in the grouping of the powder lines (d=1–3 A.). According to Hallimond, these differences, however, are not sufficient to enable precise discrimination of every chlorite and because of this the x-ray powder photograph of almost every chlorite is grouped into a type called normal chlorite type. As the x-ray powder patterns of the three species, chamosite, amesite, and cronstedite, show marked differences from each other and also from that of the normal chlorite type, in the grouping of powder lines (d=1–3 A.), only these three chlorites are discriminated by x-ray powder photographs. In Table 5, the differences between the powder photographs of chamosite and those of normal chlorite are shown. The measured spacings of powder photographs of chamosite from the Arakawa mine, shown in Table 6, agree

(22) About x-ray powder photographs of chamosite. L. Pauling, *Proc. Nat. Acad. Sci.*, **16**(1930), 578; R. C. McMurchy, *Z. Krist.*, **88**(1934), 420; A. N. Winchell, *Amer. Mineral.*, **13**(1928), 161.

(23) H. Jung und E. Köhler, *Chem. Erde*, **5**(1930), 182; H. Jung, *Chem. Erde*, **6**(1931), 275.

(24) A. F. Hallimond, *Mineralog. Mag.*, **25**(1939), 462.

with those of chamosite, given by Hallimond. No corrections were applied to the readings in Table 6, [1], [2], [3].

Table 5. Differences Between X-ray Powder Photographs of Chamosite and Those of the Normal Chlorite Type (after A. F. Hallimond).

d (A.)	Chamosite	Normal chlorite type	d (A.)	Chamosite	Normal chlorite type
2.63–2.65	+	−	2.10	+	−
2.57–2.59	−	+	2.00	−	+
2.54–2.55	−	+	1.86–1.90	−	+
2.42–2.38	−	+	1.81–1.83	−	+
2.25–2.29	−	+	1.37–1.39	−	+

+ shows the reflection from the net planes having corresponding spacings.
− shows almost absence of this reflection.

Table 6. X-ray Powder Photographs of Chamosite.

[1]			[2]			[3]			[4]	
I	$2l$ (cm.)	d (A.)	I	$2l$ (cm.)	d (A.)	I	$2l$ (cm.)	d (A.)	I	d (A.)
10	1.74	6.49	10	1.63	6.82	10	1.55	6.62	vvs	6.98
3	2.61	4.53	2	2.42	4.61	5	2.27	4.54	m	4.53
2	3.12	3.80	—	—	—	—	—	—	—	—
10	3.42	3.47	8	3.21	3.50	8	3.00	3.47	s	3.51
2	3.59	3.31	—	—	—	—	—	—	—	—
2	4.33	2.76	2	3.69	3.06	2	3.75	2.78	—	—
—	—	—	10	4.07	2.78	—	—	—	—	—
2	4.53	2.65	2	4.23	2.68	—	—	—	w	2.66
8	4.82	2.50	5	4.54	2.51	5	4.18	2.50	m	2.48
—	—	—	2	4.89	2.34	—	—	—	—	—
3	5.71	2.13	5	5.41	2.13	5	4.95	2.14	w	2.12
—	—	—	2	5.93	1.96	—	—	—	—	—
—	—	—	2	6.15	1.89	—	—	—	—	—
2	7.08	1.75	7	6.79	1.73	5	6.10	1.77	w	1.74
2	7.28	1.71	—	—	—	—	—	—	—	—
8	8.16	1.55	6	7.66	1.56	2	7.03	1.56	ms	1.55
4	8.38	1.52	3	7.87	1.53	5	7.20	1.52	m	1.52
3	9.12	1.41	2	8.52	1.43	2	7.45	1.48	—	—
—	—	—	—	—	—	2	7.85	1.42	mw	1.42
—	—	—	—	—	—	2	9.10	1.26	w	1.32
—	—	—	—	—	—	2	9.84	1.18	—	—
—	—	—	—	—	—	1	11.65	1.05	—	—
—	—	—	—	—	—	1	12.84	1.01	—	—

[1] Chamosite (Dairissikō, Tūka Province, Manchoukuo). Unfiltered Fe radiation. Camera radius 30.28 mm.
[2] Chamosite (Dairissikō, Tūka Province, Manchoukuo). Unfiltered Fe Radiation. Camera radius 30.28 mm. (Presented by Mr. Sakurai).
[3] Chamosite (The Arakawa mine, Japan). Unfiltered Co radiation. Camera radius 28.65 mm.
[4] After A. F. Hallimond, Mineralog. Mag., **25** (1939), 462, Fig. 1.
I: Intensity; d: Measured spacing; $2l$: Distance between two corresponding powder lines measured on the film.

Oscillation Photographs. For oscillation photographs, unfiltered Mo radiation with 35–45 kv. and 15 ma. is used. The exposure is about 2 hours for each experiment.

Experiment 1: The oscillation photograph was taken by mounting a narrow bundle of slender flakes that were separated from the aggregates and made to oscillate about the fibre axis, as shown in Fig. 19. On the

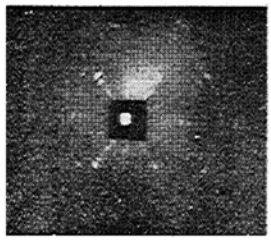

Fig. 19.

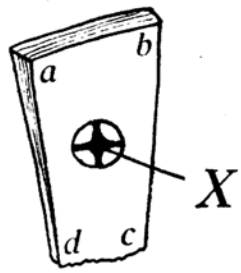

Fig. 20.

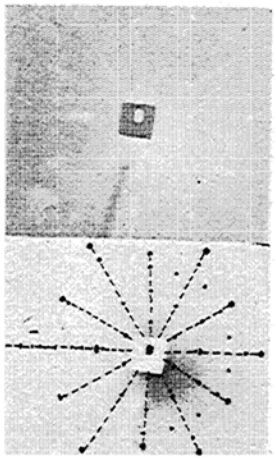

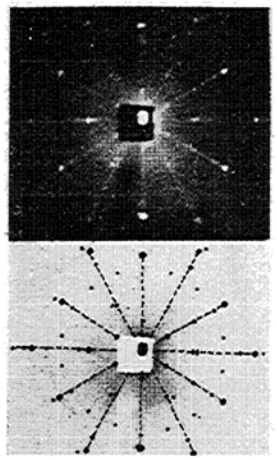

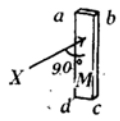

Fig. 21.

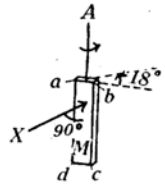

Fig. 22.

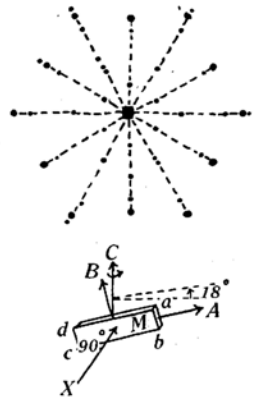

Fig. 23.

photograph, arc-shaped diffused spots arranged almost concentric to the centre of the photographic plate are recognized showing "a fibre photograph" (Fig. 19), consequently the bundle is a somewhat radial aggregate of slender crystal flakes. The measured spacing along the fibre axis nearly coincides with b_o (orthohexagonal axis) in the chlorite structure.

Experiment 2: A narrow thin tabular cleavage flake (Fig. 20) was carefully separated from the aggregates and mounted on the camera, the direction of the elongation of the slender flake coinciding with that of the oscillating axis. The x-ray beam is then directed perpendicular to the cleavage plane of the stationary flake. The photograph thus obtained is as shown in Fig. 21. Spots are seen arranged on the 6-th radiating band. The arrangement and blackening show apparent 6-th symmetry. (Fig. 21)

Experiment 3: The flake, mounted as in experiment 2, is made to oscillate 18° to one side giving the photograph shown in Fig. 22. It is notable that the pattern coincides almost perfectly with the photograph as obtained in experiment 2. The measured spacing along the direction of the oscillation axis is 9.36–9.37 A., coinciding with b_0 (orthohexagonal axis) in the chlorite structure (Fig. 22).

Experiment 4: The flake, mounted as in experiment 2, is made to turn 60° in a plane perpendicular to the direction of the x-ray beam. From this position, the flake is made to oscillate 18° to one side, giving the photograph shown in Fig. 23, which also coincides perfectly with the photographs obtained in experiments 2 and 3 (Fig. 23).

Experiment 5: The flake, mounted as in experiment 2, is made to turn 90° in a plane perpendicular to the direction of the x-ray beam, and from there the flake is oscillated 18° to one side, resulting in the pattern shown in Fig. 24. The measured spacing along the direction of the oscillation axis is 5.37–5.41 A. coinciding with a_0 (orthohexagonal axis) in the chlorite structure. Although the photograph, at a glance, differs from those obtained in the preceding experiments, when it is turned sideways, it agrees almost perfectly with the photographs obtained in the preceding experiments.

These experiments are summarized as follows:

(1) There are no differences between the photograph obtained in experiment 2 and the photograph obtained oscillating the flake, mounted first as in experiment 2, to one side from the original position where the cleavage plane of the flake is perpendicular to the x-ray beam.

(2) A flake, mounted with its flat plane perpendicular to the x-ray beam, is made to oscillate 18° to one side from the original position, and the oscillation photograph is taken. The flake is next turned at a certain angle in a plane perpendicular to the direction of the x-ray beam and made to oscillate 18° to one side from that position, and an oscillation photograph is taken. These two photographs agree with each other provided that one of them turns at the angle just mentioned.

Experiment 6: As diagramatically shown in Fig. 25, the flake is turned 45° from the original position in experiment 5, and from that new position, the flake is made to oscillate 18°, giving the photograph shown in Fig. 25. On the left-hand side half, facing the emitted direction of the x-ray beam, clear spots are seen, whereas on the right half, somewhat arc-shaped diffused spots are seen arranged concentric to the center of the photographic plate. Next, the flake is made to oscillate 18° from the position, as shown in the diagram, Fig. 26. The position is symmetrical with the original position shown in Fig. 25, about a plane which

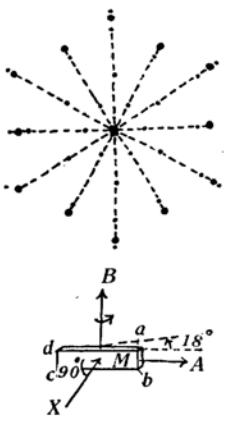

Fig. 24.

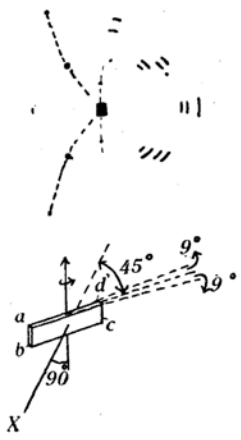

Fig. 25.

Fig. 26.

contains the oscillation axis and is perpendicular to the photographic plate. The oscillation photograph thus obtained is shown in Fig. 26, being reversed, the left being right here, as compared with the photograph in Fig. 25.

Experiment 7: The flake is set with its cleavage plane parallel to the direction of the x-ray beam, its elongation coinciding with the oscillation axis. From this position, the flake is made to oscillate 18° to one side, resulting in the photograph shown in Fig. 27, in which some of the spots are arranged in a layer-line (Bernal curves), while other spots are diffused and irregularly distributed.

Fig. 27.

Fig. 28.

Experiment 8: The flake is made to oscillate 18° about a direction perpendicular to the cleavage face, and the directed x-ray beam is parallel to the cleavage face, as shown in Fig. 28. The photograph thus obtained is shown in Fig. 28, in which most of the spots are diffused and distributed at random, except a few spots with $\xi=0$ on Bernal curves. Of these, two

intense spots with $\xi=0$ (Bernal curves) show spacing of about 7 A. on Bernal net, which is near 1/4 of c_0 in the structure of the chlorites. In all the preceding photographs, faint concentric ring reflections are always observed, corresponding to the x-ray powder photographs.

After these experiments, the flake was examined under the microscope. The appearance of the flake under the microscope is uniform, an optic elasticity axis X being almost perpendicular to the cleavage and the axial angle almost 0° to nearly 5°, but in parts somewhat differently orientated aggregates or small fibrous aggregates are seen in the flake. The characteristic x-ray photographs as obtained by the writer from the cleavage flake of chamosite were taken by Linnik, Hutton, and Hendricks with other minerals as members of the stilpnomelane group, heated mica and kaolinite etc.

Hutton[25] took the characteristic Laue photographs and unusual 15° oscillation photographs from members of the stilpnomelane group being made by oscillating about an axis in the c-plane, using iron and cobalt radiations. The Laue photographs show almost complete asterism with 6-fold symmetry. According to Hutton, the following explanations are given about the characteristics observed in these photographs; that is, the structures of these minerals are built up with distorted and disorientated mica sheets. In the structures of these minerals two-dimentional super lattices are present, and he noticed that "in the oscillation photographs obtained, the intense sub-lattice reflections are spread out along Debye-Scherrer curves and the weak super lattice spots in the c-axis oscillation photographs show smearing along the direction of the row-lines. The effect of the former indicates some disorientations of the sub-units and the effect of the latter could be produced by lack of perfect regularity in the packing of the sub-units and in the case of Laue photographs asterism would result."

Linnik[26] obtained an x-ray photograph from the heated cleavage flake of mica with copper radiation incident at the normal angle to the cleavage plane. He explained that such a cleavage flake is built up with many plates, parallel to the original cleavage surface but incorrectly spaced and that a system of spectra corresponding to a series of two-dimentional lattices is then produced in the x-ray photograph, obtained from the heated mica cleavage flake as above.

Hendricks[27] took the characteristic Lauegram with the cleavage flake of kaolinite using general radiation from an x-ray tube with a tungsten anticathode showing almost complete asterism with 6-fold symmetry. He also obtained the x-ray photographs in two cases from the kaolinite crystal, that is, in one case, the photograph is made with the stationary crystal of the kaolinite vertical and a partially monochromatic beam of MoK passing through the crystal normal to the cleavage surface and in the other, 30° oscillation photograph is made with the same crystal being placed first in the same orientation as in the former case and oscillated about an axis in the cleavage plane, and he noticed that these

(25) C. O. Hutton, *Mineralog. Mag.*, **25**(1938), 172.
(26) W. Linnik, *Nature*, **123**(1929), 604.
(27) S. B. Hendricks, *Z. Krist.*, **71**(1929), 269.

two photographs are almost identical, and are symmetrical having radial streaks with spots on them, showing apparent 6-fold symmetry. These photographs are quite similar to the photographs with the cleavage flake of chamosite obtained by the writer and also, as already noticed by Hendricks, to the x-ray photograph obtained by Linnik. Hendricks also obtained the x-ray photographs from heated or unheated cleavage flakes of mica and examined them.

According to Hendricks, the characteristics of the x-ray photographs, obtained from the cleavage flakes of kaolinite and heated mica, are not explained as a diffraction pattern of the x-ray beam from a number of superimposed two-dimentional gratings as postulated by Linnik but they are fully explained as a diffraction pattern from a characteristic micaceous crystalline aggregate, in which individual fragments are orientated at a small angle (as much as 5 degrees in this case) but are unaccompanied by the rotation about the normal to the cleavage surface.

From the above reference, it is noticed that the characteristic x-ray photographs, obtained from the cleavage flake of the chamosite by the writer, are the same type as those obtained from that of the kaolinite by Hendricks, and are fully accounted as a diffraction pattern from the characteristic crystalline aggregate explained by Hendricks as abstracted above.

Lastly the gitter constants of the chamosite are compared with those of the chlorites already obtained by other investigators shown in Table 7.

Table 7. Gitter Constants of Chlorites.

	[1] Pennine (Pauling) (A.)	[2] (McMurchy) (A.)	[3] Leuchtenbergite (Madagascar) (A.)	[4] Prochlorite (Madagascar) (A.)	[5] Clinochlore (Manchoukuo) (A.)	[6] Daphnite (A.)	Chamosite (The Arakawa mine, Japan) (A.)
a_0	5.2– 5.3	5.304– 5.352	5.35	5.38	5.36	5.40	5.37–5.41
b_0	9.2– 9.3	9.187– 9.270	9.18	9.20	9.24	9.36	9.36–9.37
c_0	14.3–14.4	28.306–28.582	28.76	28.75	28.85	28.2*	—
β	96°50′	97°8′40″	—	—	—	—	—

* Spacing perpendicular to (001).

[1] L. Pauling, *Proc. Nat. Acad. Sci.*, **16**(1930), 578.

[2]–[4] R. C. McMurchy, *Z. Krist.*, **88**(1934), 420, SB III (1936), 156 (leuchtenbergite, sheridanite, prochlorite, etc.)

[5] K. Omori, *J. Japan. Assoc. Mineral. Petrol. Econ. Geol.*, **21**(1939), 177 (in Japanese).

[6] A. F. Hallimond, *Mineralog. Mag.*, **25**(1939), 463.

A Species of Iron-rich Hydrous Silicate ("Lembergite") in Tertiary Iron Sand Beds.

Introduction. A number of iron sand beds were found in the Tertiary of Japan.

(1) Nasino, Oide-mura, Natori-gun, Miyagi Prefecture.
(2) Irisugawa, Sinti-mura, Tone-gun, Gunma Prefecture.
(3) Saruhasi, Tomihama-mura, Kita-katura-gun, Yamanasi Prefecture.

(4) Kihado, Heki-mura, Ōtu-gun, Yamaguti Prefecture.
(5) Ku-mura and Kōnan-mura, Kakeigawa-gun, Simane Prefecture.

The geological and mineralogical characteristics of these iron ore deposits are as follows:—

Geological Observations. (I) *Nasino, Oide-mura, Natori-gun, Miyagi Prefecture.* Tuffaceous rocks (tuff, tuffaceous sandstone, tuffaceous conglomerate, brecciated tuff) prevail in the entire neighbourhood of Oide-mura, Natori-gun, Miyagi Prefecture, the southern area of which is partly overlapped by a basalt flow.

These ore bodies are locally distributed in the tuffaceous rocks, near Nasino, as somewhat irregular shaped masses. In an outcrop clearly observed along a small valley on the eastern side of Nasino, an ore bed was found embedded in tuffaceous rocks, partly conformably and partly unconformably stratified with sharp boundaries to the upper and lower rock facies. Along the upper horizon of the ore bed, a fossiliferous tuffaceous conglomerate (or tuff breccia) and a glauconite(grünerde?)-bearing pumice tuff (or tuff breccia, or tuffaceous conglomerate) are found with irregular stratifications. The dip and strike as measured from a plane between a tuffaceous sandstone (or tuff) and a thin bed of conglomeratic tuff are N 60° W; 30° E near the outcrop mentioned above.

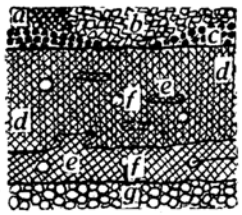

Fig. 29.

The ore is, macroscopically, a fairly loose black tuffaceous magnetite-sandstone (partly conglomeratic), consisting of crystal grains of magnetite, quartz, and pyroxene cemented by a dark green earthy mineral. Round gravels, about 2–3 cm. in diameter, of black volcanic rocks, pale greenish-coloured shale, and quartzite are sporadically found, covered by a dark green earthy mineral. The dark green tuffaceous sandstone is often found intercalating in the ore body. Usually, the ore, when exposed to sun-light tarnishes to a brownish tint, which must be caused by the tarnish of a greenish-coloured mineral included in the iron sand bed.

The rock facies near the ore body is as shown in Fig. 29.

(a) Glauconite(grünerde?)-bearing pumice tuff or tuffaceous sandstone.
(b) Glauconite(grünerde?)-bearing conglomeratic pumice tuff containing pebbles of (a).
(c) Brownish-green, magnetite bearing tuffaceous sandstone.
(d) Black tuffaceous magnetite-sandstone (main ore body).
(e) Greenish-black tuffaceous sandstone.
(f) Pebbles of pale greenish coloured quartzite.
(g) Conglomerate (tuffaceous).

(II) *Irisugawa, Sinti-mura, Tone-gun, Gunma Prefecture.*

Near Irisugawa, Sinti-mura, Tone-gun, Gunma Prefecture, tuffaceous rocks (white tuff, green tuff, tuffaceous sandstone, tuffaceous conglomeratic sandstone, and tuff breccia) prevail, intruded by small masses of olivine basalt. Along the upper horizon of the tuffaceous rocks, tuffaceous magnetite-sandstone (the ore body) is stratified almost horizontally, showing a ring-shaped outcrop at the middle of a hill near Irisugawa. Under the ore body, tuff, brown shale, a thin brown coal seam, and tuffaceous coarse-grained sandstone are observed. The ore body is a black (or brownish) hard compact tuffaceous magnetite-sandstone, showing no marked conglomeratic part, including only a few round gravels, about 5 cm. in mean diameter, covered by thin films of a dark green earthy mineral, which tarnishes to a brownish colour on exposure to the sun. Small lenticular masses of yellowish-brown, green, dark green, and white tuffaceous sandstone, consisting of sand grains cemented by a dark green mineral as described in detail in the section on the microscopic observations, are held in the iron sand bed along the bedding plane.

(III) *Saruhasi, Tomihama-mura, Kita-katura-gun, Yamanasi Prefecture.*

The area near Saruhasi, Yamanasi Prefecture, mainly consists of Tertiary sedimentaries, associated with tuff breccia, agglomerate, intruded breccia, andesite, and olivine basalt, showing an almost constant strike and dip of N 60°–70° W; 60°–70° N.

Lava flow (porous augite andesite).

T_1 Alternations of sand and gravel.

T_2 Conglomerate (alternating with thin beds of sandstone, conglomeratic sandstone, and sandy shale).

T_3 Conglomerate. *Zone of Ostrea gigas* THUNBERG. Brown coal seams. Iron sand beds. Augite basalt. Agglomerate. Tuff breccia. Intruded breccia.

T_4 Tuff. Tuffaceous sandstone. Green tuffaceous conglomeratic sandstone.

T_5 Hard sandstone. Hornfels. Quartzite.

Lava flow (Saruhasi Lava): The lava is a porous augite andesite, overlapping only the southern side of the Katura-gawa, showing beautiful columner joints only along its southern cliff.

T_1 is an alternating bed of sand and gravel, which is mostly composed of subangular pebbles of volcanic rocks and pieces of coaly wood (partly limonitized), permeated by iron ochre at several localities. It unconformably overlaps the lower rock formation. False bedding predominates.

T_2 is mainly a thick, reddish conglomerate, alternating with thin (about 0.5 m.), gray, or blackish-gray, or brownish beds of sandstone, showing an almost constant dip of 70° N and a strike of N 70°–60° W. The conglomerate is composed of round gravels of quartzite, hard sandstone, diorite, etc. (all about 10 cm. in diameter).

T_3 corresponds to the lower horizon of the T_2 horizon mentioned above. It consists in the main of a conglomerate (finer than that found in T_2), with sandstone, sandy shale, conglomeratic sandstone (gray, yellowish-gray, reddish-gray), brown coal seams, and zone of *Ostrea gigas* THUNBERG. Along the base of T_3 a dark green characteristic conglomerate called "*mame*" (beans) is distributed which is composed of very round bean-like pebbles, cemented mainly by a dark green earthy mineral. Iron sand beds are locally distributed in this bean-like conglomerate as subparallel, somewhat irregular thin lens-shaped masses, with sharp boundaries, and variable thickness. Along the lowest horizon of T_3, a thin basalt sheet is extensively distributed, presenting various aspects, the minerals held being plagioclase, augite, and magnetite. The rocks described as tuff breccia, agglomerate, and intruded breccia show reddish-brown, or greenish-gray, or blackish-gray colour, or mixtures of these colours. They consist of angular breccias of greatly altered andesite or basalt, quartzite, and sandstone, cemented by andesitic matter, showing under the microscope, flow structure in the cementing part. Large blocks of the undermentioned green conglomerate of T_4 are caught in the intruded breccia.

T_4 is an alternation of beds of pale grayish-white tuff and sandy shale above, and of beds of hard sandstone and conglomerate below, extending to N 60°–70° W, dipping 60°–70° N. This hard sandstone is mostly greenish-gray to gray alternating partly with brown tuffaceous sandstone or red cherty sandstone. The hard conglomerate is composed of subangular pebbles of medium-sized grains of green cherty sandstone.

T_5 includes quartzite, hornfels, graphite phyllite, and greenish-gray to black hard sandstone and darkish-green to gray conglomerate, extending to N 70°–90° W, with a steep dip of 70°–90° either N or S, and belonging to an old Palaeozoic formation.

(IV) *Kihado, Heki-mura, Ōtu-gun, Yamaguti Prefecture.*

In the neighbourhood of Kihado, Heki-mura, Ōtu-gun, Yamaguti Prefecture, Tertiary formations prevail, namely,

T_1 Gray of white or red { tuff, / tuffaceous conglomeratic sandstone, / tuffaceous sandstone, / tuffaceous shaly sandstone.

T_2 Alternation of { tuffaceous conglomerate or sandstone or tuffaceous sandstone or tuffaceous shaly sandstone and thin beds of brown coal or coaly tuffaceous sandstone.

T_3 { Conglomerate. / Conglomeratic sandstone. / Thin beds of tuffaceous coaly conglomeratic sandstone. / Conglomeratic tuffaceous magnetite-sandstone[28]. / Tuffaceous magnetite-sandstone. } (false beddings).

T_4 Alternation of { coarse tuffaceous conglomerate[29] with large natural coals, composed mainly of pebbles of volcanic rocks and quartzite / tuffaceous { sandstone, / shaly sandstone, / sandy shale (partly fossiliferous), / conglomeratic sandstone.

The iron sand bed is found in conglomerate as small and almost parallel lenticular masses with sharp boundaries. In an outcrop clearly observed along the coast, north of the station of Kihado, the upper part of the iron sand bed is in contact with a thin brown coal seam (5–10 cm. thick) or with tuffaceous sandstone (partly conglomeratic). The ore body, horizontally, transits somewhat abruptly to a conglomerate without any magnetite grains, showing variable strikes, dips (for example, N 20° E, 10° N; NS, 10° W; N 30°–40° W, 10° S, etc.) and thicknesses. The iron sand bed and rock formation under it are penetrated by small calcite veins, carrying small pieces of pyrite or chalcopyrite, which often impregnate the iron ore bed as small crystal grains. The ore body is, macroscopically, a dark green conglomeratic magnetite-sandstone, or dark green tuffaceous magnetite-sandstone, composed of fine grains of magnetite, augite, feldspar, and round gravels of volcanic or sedimentary rocks about 1–0.5 cm. in diameter, all of which are cemented by a dark green earthy mineral.

(V) *Ku-mura and Kōnan-mura, Kakeigawa-gun, Simane Prefecture.*

The geological observations in the neighbourhood of Ku-mura, Simane Prefecture are summarized as follows:—

T_1 { Sandstone. Conglomerate. / Limonite sandstone. / Limonite conglomerate. / Limonite bed. / Gray sandy shale. } { Limonite veins. / Linomite concretions (sphere, rode and other irregular shapes). }

---

(28) Very similar to the conglomerate at Saruhasi (*"mame"*).
(29) Fossiles are rarely found; but their species are not yet determined.

T_2	Brownish-gray sandstone (partly conglomeratic). Thin limonite sandstone. Hard fossiliferous sandstone.	Alternation of iron sand beds, brownish-gray sandstone (partly conglomeratic) and thin limonite sandstone.	Conglomerate with large pebbles. Conglomeratic sandstone. Sandstone. Iron sand bed. Dark greenish-gray to gray sandstone. Grayish-green tuffaceous sandstone.

As shown above, this rock formation is classified into two main zones. The upper zone (T_1) is characterized by limonite, which cements the grains of sandstone or conglomerate, and is partly found as the somewhat enriched part being parallel to the bedding plane (limonite beds) or cutting the plane (limonite veins), or is found partly as concretions. False beddings predominate, and various, oddly-shaped

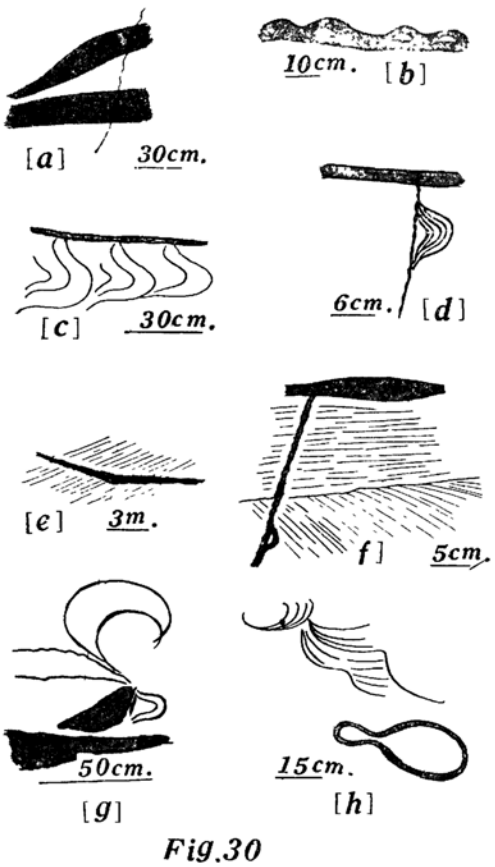

Fig.30

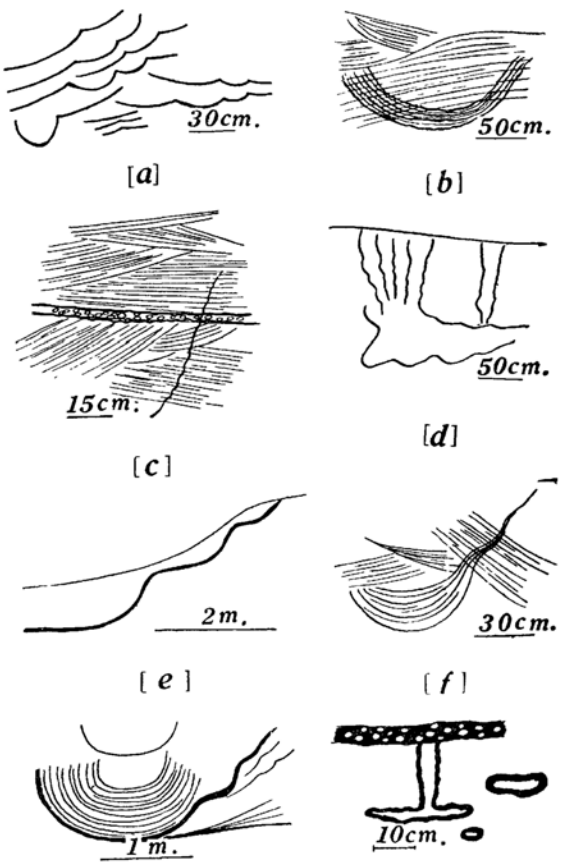

Fig.31

Fig. 30, and Fig. 31.
Odd-shaped limonitized bands observed in the Tertiary sandstone at Ku-mura, in Simane Prefecture.

limonitized bands are observed, some of which are shown in Figs. 30, 31. In the lower zone (T_2) thin limonitized beds, about 1 to 2 cm. thick, are found locally, alternating with brownish-gray sandstone, but showing a more regular alternation comparing with the limonitized zones in the upper part. False beddings do not predominate here.

A very hard fossiliferous sandstone (EW in strike, 10° N in dip) is locally distributed, alternating with a loose, brownish-gray sandstone. In the latter fossils are also rarely found, being replaced partly or wholly by limonite. Iron sand beds are also locally distributed near Koganeyama and Hatadani. The formation that accompanies the main iron sand beds is an alternation of conglomerate with very large pebbles (20–30 cm. in mean diameter), and sandstone and a grayish-green tuffaceous sandstone. The dip and strike of these iron sand beds are N 70°–80° E; 10°–20° N. Natural coal is also found in the iron sand beds. In the iron sand beds in Hatadani, network veins of calcite, crusts or oolites of opal, and silicified woods are found. As stated above, magnetite grains are concentrated locally, forming iron sand beds, but in the sedimentaries of the lower zone, magnetite grains are extensively contained. The iron sand beds at Anedani are somewhat irregular masses at the upper part of the lower zone (T_2). The ore bodies are stained by limonite, and pieces of brown carbonized plants, silicified woods, crusts or oolites of opal are detected in the ore bodies.

(VI) *Geological ages.*

As just mentioned, fossiliferous zones accompany the iron sand beds of Saruhasi, Kihado, and Ku-mura. The fossils have been determined by Dr. Y. Otuka, of Geological Institute, Imperial University, Tokyo, as follows:—

Saruhasi:

Ostrea gigas THUNBERG (Lowest pliocene).

Kihado:

Acila mirabilis var. ashiyaensis (NAGAO)
Venericardia subnipponica NAGAO
Polinices euspira ashiyaensis NAGAO
} (Concentrated partly in tuffaceous sandy shale) (Upper oligocene)

Ku-mura:

Dosinia sp. (aff. nomurai OTUKA)
Maktra sp.
} (Middle miocene)

Judging from the relation between the horizons of the iron sand beds and the fossiliferous zones and the ages of the latter, as mentioned above, all the above three iron sand beds were formed during middle miocene.

(VII) *Summary of the geological observations.*

The foregoing geological observations may be summarized as follows:

(1) The ore bodies are always enclosed in tuffaceous rocks (tuffaceous sandstone, tuffaceous conglomerate, or tuff) as subparallel and somewhat irregular small lens-shaped masses with sharp boundaries, extending to the bedding planes.

(2) The ore body is a part of the tuffaceous rocks, that is, mainly black tuffaceous magnetite rocks, which are usually composed of small grains of magnetite, feldspar, and augite, and round pebbles of volcanic rocks, quartzite, sandstone etc., and all of them are mainly cemented by greenish-coloured (dark green or dirty green) earthy minerals.

(3) The ore bodies are always somewhat greenish-coloured (dark green or dirty green) masses, owing to the presence of intimately associated greenish-coloured earthy minerals, which often tarnish to a brownish colour after exposure to sun-light, and the greenish-coloured (dark green or dirty green) tuffaceous sandstone or conglomerate is always found accompanying the ore bodies.

(4) The ore bodies are often penetrated by very narrow veins of calcite, with pyrite or chalcopyrite. Calcite also forms the binding material for

the mineral grains of the iron ore. Silicified woods, natural carbons, limonitized plants or fossils, brown coal seams, and nodules of limonite are often found near the iron sand beds.

(5) From the fossils found in the beds accompanying the iron sand beds in a number of localities, most of the ore beds seem to have been formed during middle miocene.

(6) The iron sand beds in the Japanese Tertiary, are sediments of shallow sea or lagoon area, and most of them have been deposited during middle miocene.

Microscopic Observations. (I) *The ore from Nasio, Miyagi Prefecture* (Fig. 32): This ore is mostly magnetite (M) (0.2 mm. in mean diameter) and augite grains (A) cemented by volcanic glass (S) and a minute green mineral. The augite grains are replaced partly by volcanic

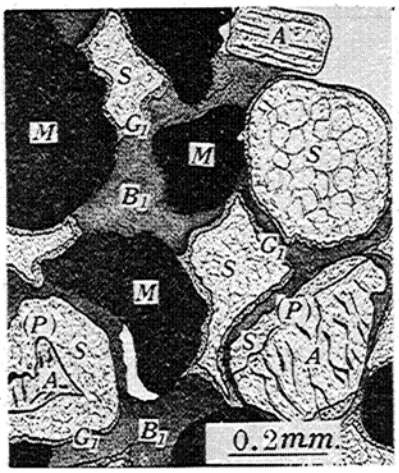

Fig. 32 (a).

Microscopic feature of dark green tuffaceous magnetite-sandstone (Nasino, Miyagi Prefecture).

M: Magnetite. S: Glass. A: Augite.
B_1: Brown mineral cementing interspaces of grains.
G_1: Green mineral surrounding mineral grains.
(P): Parts of augit grains replaced by glass partly.

(The Brown and green mineral in the speciemen are not determined owing to their minuteness.)

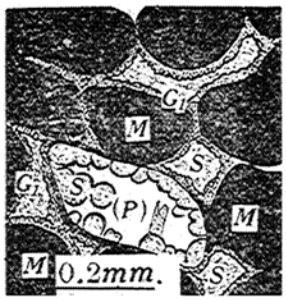

Fig. 32 (b).

Microscopic feature of dark green tuffaceous magnetite-sandstone (Nasino, Miyagi Prefecture).

M: Magnetite. S: Glass.
G_1: Green mineral.
(P): An augite grain replaced by glass.

(The green mineral in the speciemen is not determined owing to its minuteness.)

glass (as in Fig. 32, (b)), most of which are optically isotropic. showing an oolitic texture in the interstices of the mineral grains. Quartz, partly chalcedonic, is found associated with the cementing volcanic glass. The green mineral (0.01 mm. in mean size) is an aggregate of very minute grains always surrounding magnetite and other mineral grains (G_1, Fig. 32). The brown perfectly optically isotropic mineral is partly found

filling the interstices of the mineral grains. These two minerals, green and brown, may be of different species, but their properties have not yet been precisely determined owing to their minuteness.

The dark green tuffaceous sandstone, intercalated in the ore bodies, is composed of grains of plagioclase, augite, pieces of altered andesite quartzite, sandstone (all 0.2 mm. in mean diameter), cemented by the brown to greenish-brown earthy mineral, which closely resembles that found in the Kihado or Saruhasi ores to be mentioned later.

(II) *The ore from Irisugawa, Gunma Prefecture* (Fig. 33): The ore mostly consists of magnetite grains (0.2 mm. in mean size) cemented by quartz grains (0.1 mm. in mean size) and a green mineral (G_2). The

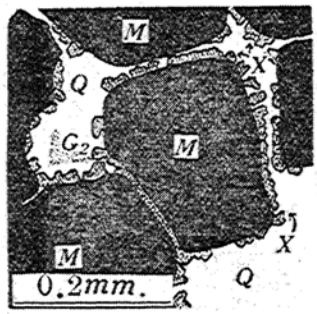

Fig.33(a)

Microscopic feature of tuffaceous magnetite-sandstone (Irisugawa, Gunma Prefecture).
M: Magnetite. Q: Quartz.
X: A mineral undetermined.
G_2: Green mineral.
(The green mineral in this speciemen is not determined owing to its minuteness.)

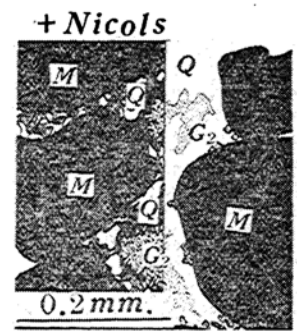

Fig.33(b)

Microscopic feature of tuffaceous magnetite-sandstone (Irisugawa, Gunma Prefecture).
M: Magnetite. Q: Quartz.
G_2: Green mineral.
(The green mineral in this speciemen is not determined owing to its minuteness.)

latter mineral (G_2) occurs as very minute scales (pleochroism indistinct) in the central parts of the interstices of the mineral grains (G_2, Fig. 32, (a), (b)). Owing to its minuteness the properties of the green mineral have not yet been precisely determined. It is very characteristic that small zircon- or rutile-like mineral grains (0.02 mm. in mean diameter) surround the magnetite grains as an accessory mineral (X, Fig. 33, (a), (b)).

The dark green tuffaceous sandstone, intercalated in the ore bodies, is composed of augite, plagioclase, quartz, hornblende, and pieces of altered volcanic rocks, cemented by a brownish-green earthy mineral (0.01 mm.), and its properties are estimated by the methods to be described later.

(III) *The ore from Saruhasi, Yamanasi Prefecture* (Fig. 34): Most of the ore consists of grains of magnetite and augite, associated with fragments of quartz, feldspar, zeolite-like minerals, altered basalt, quartzite, and sandstone, the whole being cemented by a brown to greenish-brown mineral (B_3) or partly by clacite (C). The brown to greenish-brown mineral either fills the interstices of the mineral grains

mentioned above (5, Fig. 34) or surrounds them as narrow band-like aggregates, as shown in 2, Fig. 34. Some augite grains are replaced, starting from their cleavage cracks, partly by the brown to greenish-brown mineral (in the extreme cases a whole grain is often perfectly replaced), while some are replaced by calcite, starting from their outer parts, leaving behind rings of the brownish mineral in the calcite masses as seen from 3, 4, Fig. 34. The dark conglomeratic parts are composed of round small pebbles of quartzite, sandstone, and altered volcanic rocks, cemented mainly by the brownish mineral mentioned above, which also covers the surface of the pebbles as thin films.

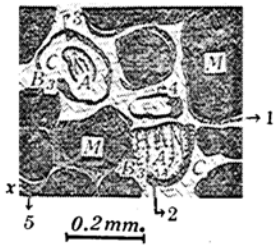

Fig.34

Microscopic feature of dark-green tuffaceous magnetite-sandstone (Saruhasi, Yamanasi Prefecture).

M: Magnetite. A: Augite. C: Calcite.
B_3: Brown mineral ("lembergite").

The properties of the brown to greenish-brown mineral are estimated by the methods to be mentioned later.

(IV) *The ore from Koganeyama, Simane Prefecture* (Fig. 35): This ore is a dirty green or dark green tuffaceous sandstone, consisting

Fig.35(a)

Microscopic feature of dirty green tuffaceous magnetite-sandstone (Koganeyama, Simane Prefecture).

M: Magnetite. A: Augite.
F: Plagioclase.
B_4: Green mineral ("lembergite") of Type 1 (surrounding grains).
G_4: Green mineral ("lembergite") of Type 2 (cementing interspaces of grains).
1: Features of green mineral ("lembergite") of Type 1.
2: Oolitic texture of green mineral ("lembergite") of Type 2.

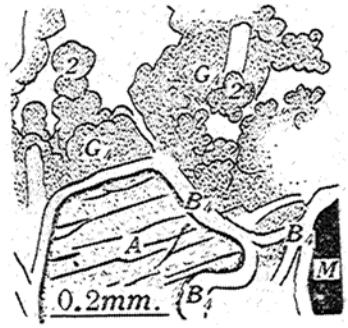

Fig.35(b)

Microscopic feature of dirty green tuffaceous magnetite-sandstone (Koganeyama, Simane Prefecture).

M: Magnetite. A: Augite.
B_4: Green mineral ("lembergite") of Type 1 (surrounding grains).
G_4: Green mineral ("lembergite") of Type 2 (cementing interspaces of grains).
2: Oolitic texture of green mineral ("lembergite") of Type 2.

of magnetite grains as the main component, and of quartz, feldspar, augite, epidote, and pieces of hornfels and altered volcanic rocks (all 0.2 mm. in mean size) as accessories. All these are mainly cemented by a greenish-coloured mineral, which, under the microscope, shows two kinds of appearance, one of which (Type 1) is pale brownish-green to pale greenish-brown, optically almost an isotropic mass, always surrounding mineral grains as narrow band-shaped aggregates (B_4, Fig. 35 (a), (b)) and the other, (Type 2) green minute optically anisotropic scales or fibres (0.01 mm.) either filling the interstices of the mineral grains or replacing some augite grains. The green mineral of Type 2 often shows an oolitic texture at the central parts of the interspaces in the mineral grains (G_4 Fig. 35, (a), (b). These two types of occurrence of the greenish mineral are also noticed in the ores from Hatadani and Kihado, to be stated below. Usually, in these ores, the greenish-coloured minerals of the two types just mentioned are in contact having sharp boundaries, but in a part of the ore from Hatadani, they gradually, merge together while in the Kihado ore, the greenish mineral of Type 1 is often lacking. Generally, the size of the greenish mineral of Type 2 is larger in the central parts of the interspaces of the mineral grains than around the mineral grains. From these facts, the writer concludes that these two types of greenish mineral do not essentially differ, that is, the apparent differences are the result of differences in the size of the flakes, and that Type 1 may be an aggregate of extremely fine flakes of the same mineral as that of Type 2.

(V) *The ore of Hatadani, Simane Prefecture* (Fig. 36): This ore consists of magnetite and augite grains (both 0.2 mm. in mean size), cemented by opal and a greenish mineral (0.01 mm. in mean size). As in the Koganeyama ore, there are two types of the greenish mineral, (Type 1....B_5, Fig. 36 (a), (b), and Type 2....G_5, Fig. 36, (a), (b)), which are usually found to be in contact having sharp boundaries, and are partly found to be gradually merging together. Some of the augite grains are replacd by opal or by the greenish mineral or by both of them

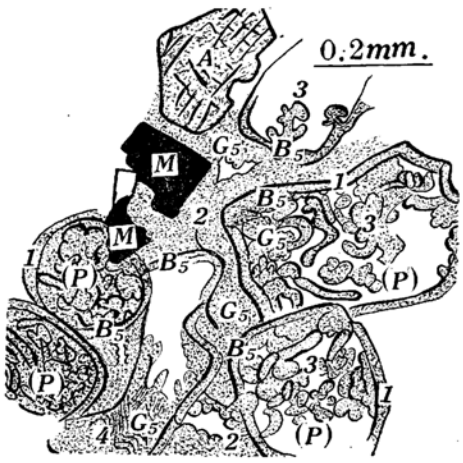

Fig.36(a)

Microscopic feature of dirty-green tuffaceous magnetite-sandstone (Hatadani, Simane Prefecture).

M: Magnetite. A: Augite.
(P): Augite graines replaced by green mineral (Type 2).
B_5: Green mineral ("lembergite") of Type 1 (surrounding grains).
G_5: Green mineral ("lembergite") of Type 2 (cementing interspaces of grains).
1: Features of green mineral ("lembergite") of Type 1.
2: Oolitic texture of green mineral ("lembergite") of Type 2.
3: Very fine fibers of green mineral ("lembergite") of Type 2 replacing augite grains.

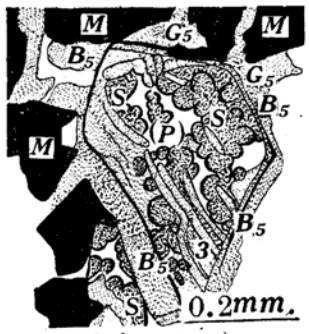

Fig.36(b)

Microscopic feature of dirty-green tuffaceous magnetite-sandstone (Hatadani, Simane Prefecture).

M: Magnetite. S: Opal.
B_5: Green mineral ("lembergite") (surrounding grains, brownish-green).
G_5: Green mineral ("lembergite") of Type 2 (cementing interspaces of grains).
(P): An augite grain replaced by opal and green mineral ("lembergite") of Type 2.
3: Fine fibers of green mineral ("lembergite") of Type 2. The green mineral ("lembergite") replacing augite grains belongs to Type 2.

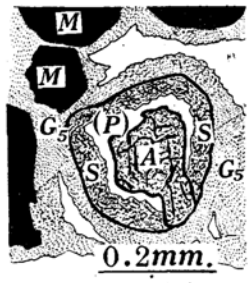

Fig.36(c)

Microscopic feature of dirty-green tuffaceous magnetite-sandstone (Hatadani, Simane Prefecture).

M: Magnetite. S: Opal.
A: Augite.
G_5: Green mineral ("lembergite") of Type 2 (cementing interspaces of grains).
(P): An augite grain replaced by opal from its outer part.

(P, Fig. 36, (a), (b), (c)). The properties of the greenish-coloured mineral are estimated by the methods to be stated below.

(VI) *The ore of Anedani, Simane Prefecture*: This ore consists mostly of magnetite grains and small quantities of augite grains (the whole 0.2 mm. in mean size), cemented by either volcanic glass or opal, the latter completely replacing some augite grains, displaying the features of chalcedonic quartz.

(VII) *The ore from Kihado, Yamaguti Prefecture* (Fig. 37): This ore which closely resembles that of Saruhasi, consists of grains of magnetite, augite, feldspar, pieces of altered volcanic rocks, sandstone, and quartzite, the whole being cemented by a brown to greenish-brown mineral (0.02 mm.) or quartz grains (0.1 mm. in mean size). The conglomeratic part of the ore bodies is mostly pebbles of altered volcanic rocks and sandstone bound by the brownish mineral mentioned above. Optically the brownish mineral is found to be anisotropic fibrous flakes (0.02 mm. in mean size) filling the interspaces of the mineral grains (G_7, Fig. 37, (b)), but an optically almost isotropic brown mineral is partly seen as narrow bands surrounding the mineral grains (B_7, Fig. 37 (b)). The brown mineral of the latter type, owing to its minuteness, has not yet been precisely identified. The brownish mineral of the former type is always found as cementing matter to a moderate extent, and selecting some parts of the ore cemented only by the former, the properties of the former brownish mineral are estimated by methods to be mentioned later.

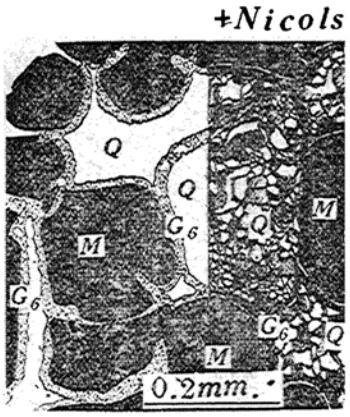

Fig. 37 (a).

Microscopic feature of tuffaceous magnetite-sandstone (Kihado, Yamaguti Prefecture).

M : Magnetite. Q : Quartz.
G_6 : Green mineral.

(The green mineral in this speciemen is not determined owing to its minuteness.)

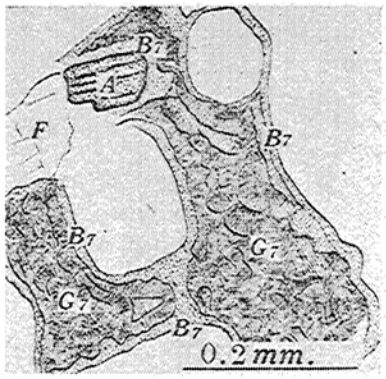

Fig. 37 (b).

Microscopic feature of dark green tuffaceous magnetite-sandstone (Kihado, Yamaguti Prefecture).

A : Augite. F : Plagioclase.
B_7 : Brown mineral (surrounding grains).
G_7 : Brown mineral ("lembergite") (cementing interspaces of grains, note vermicular forms).

In the part where the quartz grains predominate as the cementing matter, magnetite grains are surrounded by narrow banded aggregates of a green mineral (G_6, Fig. 37(a)) that differs from the above mentioned brownish minerals. Owing to its minuteness, however, the properties of this green mineral have not yet been precisely determined.

(VIII) *Summary of the microscopic observations.* From the microscopic observations mentioned above, the general properties are summarized up as follows:—

(1) As already noticed in the microscopic observations, greenish-coloured (dark green or dirty green) minerals are always intimately associated with the ore body, but under the microscope, the greenish coloured mineral often gives a brownish to brown colour as well as greenish one.

(2) Under the microscope, the ores are generally composed of grains of magnetite, augite, feldspar, and quartz, and pieces of altered volcanic rocks, sandstone, hornfels, quartzite, etc., (all about 0.5 mm. in diameter), cemented by greenish to brownish coloured minerals, quartz grains, opal, and calcite. Of these, although calcite and opal are also often found as capillary veins or fissure-filling matter, the greenish to brownish minerals never occur as vein-like matter.

(3) The greenish coloured minerals, under the microscope, often show two types of appearance; the one optically isotropic, uniform, ring-shaped, and surrounding the mineral grains in which almost neither flakes nor fibres can be discriminated, and the other an aggregate of relatively large flakes or fibres, filling the interstices of the mineral grains. In most cases these two kinds of greenish minerals are intimately asso-

ciated, and are in contact with each other having sharp boundaries, although in places, these minerals either gradually merge together, or the mineral of Type 1 is entirely lacking. The colour of the mineral of Type 1 is always more brownish than that of Type 2, and the size of the mineral flakes or fibres of the mineral of Type 2 is larger in the central parts of the interspaces of mineral grains and in replaced parts of augite grains etc. than around mineral grains. The writer is of the opinion that the apparent difference of the greenish minerals is most probably due largely to the degree of minuteness of the crystal flakes, and that the greenish mineral of Type 1 may be an aggregate of extremely fine flakes of the same mineral as that of Type 2.

(4) Augite grains are frequently replaced by the greenish to brownish minerals, calcite, quartz, or opal. Rings of the greenish to brownish minerals are often isolated in calcite or quartz masses. Chalcedonic quartz is often found associating with opal.

(5) Under the microscope, the greenish to brownish-coloured minerals are easily discriminated from serpentine or chlorites.

(6) Finally, all these iron ore bodies show altered features due to the action of hot springs in the last stage of volcanic activity. Under the microscope, the greenish to brownish coloured earthy minerals mentioned above seem to be an altered product from mafic minerals, in this case, chiefly augite grains.

On the Properties of the Greenish Coloured Mineral Associated with the Tertiary Iron Sand Beds in Japan. (I) *Introduction.* As stated above, in Japan, the greenish-coloured minerals are always found in the Tertiary iron sand beds. As some of them are extremely fine and contained in a very dispersed state their properties are not precisely determined but the greenish-coloured minerals in the following six specimens are found to be somewhat large crystal flakes and are contained in a somewhat concentrated state.

Specimen (1) A dark green mineral in the ore (dark green tuffaceous magnetite-sandstone or dark green conglomerate "*mame*") at Saruhasi. (Fig. 34)

Specimen (2) A dark green mineral in the ore (dark green tuffaceous magnetite-sandstone or dark green conglomerate) at Kihado. (Fig. 37(b))

Specimen (3) A dark green mineral in dark green tuffaceous sandstone in the ore body at Nasino.

Specimen (4) A dark green mineral in the dark green tuffaceous sandstone in the ore body at Irisugawa.

Specimen (5) A dirty green mineral in the ore (dirty green tuffaceous magnetite-sandstone) at Koganeyama. (Fig. 35, (a), (b))

Specimen (6) A dirty green mineral in the ore (dirty green tuffaceous magnetite-sandstone) at Hatadani. (Fig. 36, (a), (b), (c))

The writer first examined the optical properties of the greenish-coloured minerals in the above six specimens and next concentrated the above minerals isolating them as purely as possible using various methods to be mentioned in detail later, and examined the chemical properties and

x-ray powder photographs of these minerals, then finally concluded that all the greenish coloured minerals contained in the above six specimens belong to the same species, one of alteration products from augite described by Lemberg[35].

The writer will refer to the mineral "lembergite".

(II) *Optical properties.* As the first step, the optical properties of the greenish coloured minerals in the above six specimens were determined as shown in Table 8.

Table 8.

Specimen	Pleochroism	Refractive indices	Double refraction	Mean size
(1)	Z...greenish-brown to dark brown X...green to greenish-brown	1.56–1.58	0.02 –0.03	0.02 mm.
(2)	Z...greenish-brown X...brownish-green	1.57–1.58	0.02 –0.03	0.02 mm.
(3)	Z...greenish-brown X...brownish-green	1.56–1.58	0.02 –0.03	<0.01 mm.
(4)	Z...green to brownish-green X...pale green	1.57–1.58	0.02 –0.025	0.01 mm.
(5)	Z...green X...pale green	Indistinct	0.015–0.02	0.01 mm.
(6)	Z...green X...pale green	Indistinct	0.015–0.02	<0.01 mm.

In these optical constants thus obtained and in their appearances under the microscope, these minerals do not perfectly agree with each other, that is they are classified into three types: Type (1), the greenish minerals from Saruhasi, Kihado, and Nasino; Type (2), the green mineral from Irisugawa, and Type (3) the green minerals from Koganeyama and Hatadani. Though, under the microscope, they do not perfectly agree in appearance, from their chemical analyses and x-ray photographs, these greenish minerals in the six specimens just mentioned all belong to the same type as shown below. Consequently the differences in the optical properties of such minute minerals and in their appearances under the microscope do not show that they are essentially different.

(III) *Chemical properties.* Thin slices of the foregoing specimens, after removing the cover glasses, were immersed in warm dilute hydrochloric acid for about 1 minute, washed with distilled water, dried, then examined under the microscope, when the greenish minerals (the colour under the microscope is often brownish) were found to be skeleton crystals of colourless silica gels with low refractive indices, owing to the fact that the bases are easily and perfectly extracted, and that phenomena has already been reported on some hydrous silicates, such as zeolite and glauconite[39]. According to these literatures, extinction positions and axial

(30) E. H. Bailey, *Am. Mineral.*, **26**(1941), 565; K. Smulikowski, *Mineralog. Abstracts.*, **6**(1936), 345; F. Linne, *Fortschr. Mineral. Krist. Petrog.*, **3**(1913), 159.

angles were still preserved in the skeleton crystals of the silica gels obtained from some hydrous silicates after extracting the bases. The writer also examined the chamosite from the Arakawa mine, manganiferous thuringite from Toyama Prefecture, and other like minerals, and noticed that these minerals are also easily altered to skeleton crystals of silica gels, and in somewhat large crystal flakes, the extinction positions are clearly maintained, although the maintenance of the axial angle could not be clearly observed. The writer also noticed that such iron-rich members as iron chlorite, iron serpentine (greenalite, etc.), lepidomelane, etc., are more easily decomposed by hydrochloric acid than those poor in iron, and that, generally, the very minute crystal flakes of these minerals found in the iron ore bed are more easily attacked by acid than the large crystal flakes of the same minerals found in the veins. As a rule, it was not possible to determine precisely the properties of the greenish-coloured earthy minerals in sandstone, tuff, etc., owing to the great difficulty of separating perfectly the very minute flakes or fibres from other substances, but these greenish minerals are usually easily decomposed by warm dilute acids leaving behind colloidal silica as mentioned above, then if the mineral grains mixed with the greenish mineral are not thoroughly decomposed by dilute acids, the greenish mineral alone is easily extracted by acids. In this case, although the amounts of SiO_2 and H_2O could not be clearly determined, the amounts of bases thus extracted may be sufficient to indicate a part of the composition of the greenish-coloured earthy mineral. The foregone method is nothing but a chemical separation of minerals by acid extraction, a method already in use by a few investigators[31] in studies of earthy minerals in sedimentary rocks.

The writer concentrated the greenish-coloured minerals in the above specimens as purely as possible by the methods now to be mentioned, in order to estimate the compositions of these greenish minerals from their soluble parts extracted by warm dilute hydrochloric acid.

(IV) *Preparation of the sample for chemical analysis.* The specimen is crushed and passed through a 100-mesh sieve plate, after which the greenish minerals are somewhat concentrated into a fine powder, owing to their being soft and minute crystal flakes. The fine powders thus obtained are placed in distilled water, stirred, and separated into two parts, one a very fine powder suspended in water, and the other a relatively coarse part that rapidly falls down. In this case, the suspended fine powder is left to stand for about 5 minutes, then filtered off and dried. In this fine powder, the greenish mineral and plagioclase are mostly concentrated, the bulk of the heavy mineral grains being eliminated. This is the first stage of concentration. For comparison, the fine powder thus obtained from the specimen from Kihado was analysed (Table 9, III). Next, the relatively coarse powder which fell down rapidly in the preceding treatment, is filtered off and dried. The magnetite grains are eliminated from the powder with the aid of a hand magnet. This is the second stage of concentration whence, for comparison, the powder thus obtained from the specimens from Saruhasi, Kihado and Irisugawa

(31) T. Deans, *Geol. Mag.*, **71** (1934), 49; A. F. Hallimond, *Mineralog. Mag.*, **25** (1939), 441.

were analysed chemically, as shown in Table 9, I, II, III. The last stage of concentration of the greenish coloured minerals now follows: The powder, concentrated with the greenish mineral in the second stage as stated above, is treated with a magnetic separator, and the powder accumulated in the non-magnetic part of the magnetic separator is taken, in which the magnetite grains are perfectly eliminated, as also most of the augite grains. Lastly, the powder thus obtained is placed on a paper pasted on a flat wooden plate. When the plate, inclined about 30°, is tapped, the powder on it gradually moves down. In this case, the flaky minerals, in general, adhere readily to the paper, whereas, the crystals or grains of like size are mostly thrown down, after which the powder adhering to the paper is scraped off. In the powder thus obtained, the greenish mineral is concentrated to the purest possible state. This is the last stage of concentration. To the greenish mineral in each of the above specimens (1)–(6), which is now concentrated to the purest possible state, the following chemical test is applied. The mineral compositions of the powder thus prepared and chemically analysed were roughly determined as shown in Table 9, [4].

(V) *Qualitative tests.* (1) When the powder obtained by the foregoing preparations is treated with dilute hydrochloric acid (1:1) on a water-bath for about from 30 to 100 seconds, the greenish coloured mineral is very easily decomposed, leaving behind the white colloidal silica, the other grains being almost unaffected. From the dissolved portion iron, calcium, magnesium, and aluminium are always detected, their weight ratios being invariably $Fe_2O_3 > MgO \fallingdotseq Al_2O_3 > CaO$, while the amounts of the alkalies are negligible.

(2) When the powders obtained by these preparations are heated in a closed tube, large quantities of water are expelled. Since the mineral grains mixed with the greenish-coloured mineral in the powder are species having very little or no water of crystallization, the bulk of water expelled from the powder heated in the closed tube must have come from the greenish mineral.

(3) As already stated in the geological observations, the conglomeratic part of the ore body is composed of pebbles covered with thin films of the dark greenish mineral, showing a dark green colour. These dark green pebbles were collected and heated in a closed tube, when large quantities of water were always expelled. These pebbles were next collected and treated with dilute hydrochloric acid on a water-bath for about from 30 seconds to 1 minute, the dark green mineral covering the pebbles as thin films being easily decomposed by the acid, leaving behind thin layers of colloidal silica. From the dissolved part, iron, calcium, magnesium, aluminium and negligible quantities of alkalies are always detected, their weight ratios being $Fe_2O_3 > MgO \fallingdotseq Al_2O_3 > CaO$. From the foregoing qualitative tests, we found that the greenish-coloured mineral is a hydrous silicate of iron, aluminium, magnesium and calcium, easily decomposed by warm dilute hydrochloric acid.

(VI) *Quantitative analyses.* As indicated in Table 9, [4], the powder prepared as stated above consists mostly of the greenish mineral with some feldspar and augite. Since the last two are scarcely decomposed by the warm dilute hydrochloric acid treatment, the writer tried to esti-

mate the constitution of the greenish mineral by the method of acid extraction stated above.

(1) About 2–3 g. of the powder prepared for the qualitative tests are weighed after drying at 100–110°C and treated with dilute (1:1) hydrochloric acid on the water-bath for about from 30 seconds to 1 minute.

(2) The insoluble part that is filtered and dried at 100 to 110°C. and weighed as insoluble matter, is composed of grains undissolved by the dilute hydrochloric acid treatment just mentioned, and of the colloidal silica that separated out from the greenish mineral. The insoluble matter is ignited and weighed as "ignition loss of insoluble". Since the mineral grains not decomposed by this treatment have very little or no water of crystallization, the ignition loss of the insoluble matter is almost entirely due to the water derived from colloidal silica.

The study of the chemical composition of the colloidal silica, left behind from the low temperature hydrous silicate by the acid treatment just mentioned, is very interesting, but at the same time very difficult. The chemical compositions of the colloidal silicas left behind by the method of acid extraction from the chlorites, serpentines, etc. have already been described in the chemical literature(32). Although the chemical composition of the colloidal silica that separates out from the above mentioned greenish mineral is unknown, if it were possible to determine it by some other method, there would be no difficulty in estimating the amount of the silica in the mineral, in this case, from the amount of the ignition loss from the insoluble matter.

(3) The soluble parts, namely, soluble silica, iron, aluminium, calcium, magnesium, and the alkalies are determined by the usual analytical methods, and the alkalies are determined by the method used for soil analysis.

(4) Ferrous iron is determined by a simple method from the original powder as $(FeO)_M$ and from the insoluble part dried at 100°–110°C. as $(FeO)_I$, then $(FeO)_M-(FeO)_I$ roughly corresponds to the FeO in the soluble part. The total amount of iron in the soluble part is determined by titration, after which the ferric iron in the soluble part is estimated.

(5) The ignition loss of the original powder dried at 100°–110°C. is determined. As already stated, mineral grains other than the greenish mineral, contained in the powder, are almost all anhydrous, and the ignition loss thus obtained is mainly due to the water of crystallization of the greenish mineral. Thus, although the amounts of SiO_2 and H_2O are not clearly determined, those of Al_2O_3, Fe_2O_3, FeO, CaO, MgO, and the alkalies are determined in the soluble part, the chemical composition of which may indicate one part of the composition of the greenish mineral in the above mentioned case.

(VII) *The results.* The chemical analyses attempted with the samples prepared as stated above are given in molecular ratios (MgO as 1.00) in Table 9, [5]. As already mentioned, usually in preparing the samples analysed, the magnetic separator was used, and tapping tried, but in a few cases, for the sake of comparison, the samples were prepared by using only a hand magnet or by resorting to washing with water as shown in Table 9, I, II, III, VI.

(32) J. W. Mellor, "A Comprehensive Treatise on Inorganic and Theoretical Chemistry," Vol. 6, 294, London (1930).

Table 9. Chemical Composition of "Lembergite".

[1] Specimens	[2] No. of analysed samples	[3] Processes for the preparation of analysed samples				[4] Mineral composition estimated under the microscope				[5] Compositions of the part dissolved by hot dilute hydrochloric acid (The molecular ratio MgO : 1.00)						
		Hand magnete	Magnetic separator	Water washing	"Tapping"	Grains of "lembergite"	Grains of plagioclase	Grains of augite	Grains of opal	Al_2O_3	FeO	MgO	CaO	SiO_2	H_2O (+)	$\frac{Fe_2O_3}{FeO}$
(1) Saruhasi	I	○	×	○	×					0.47	1.43	1.00	0.70	x	1.88	Fe^{III}/Fe^{II} 2.7
(2) Kihado	II	○	×	○	×					0.39	1.06	1.00	0.26	x	1.80	0.79
	III	×	×	○	×					0.39	1.10	1.00	0.26	x	1.79	1.04
	IV	×	○	×	○	ca. 80	ca. 20	<1	non.	0 40	0.85	1.00	0.26	x	1.79	1.56
(3) Nasino	V	×	○	×	○	ca. 90	ca. 10	ca. 1	non.	0.37	0.84	1.00	0.15	x	1.70	3.40
(4) Irisugawa	VI	○	×	○	×					0.40	0.67	1.00	0.27	x	2.12	
	VII	×	○	×	○	ca. 50	ca. 30	ca. 20	non.	0.37	0.71	1.00	0.20	x	1.92	1.44
(5) Koganeyama	VIII	×	○	×	○	ca. 90	<1	<1	ca. 10	0.36	0.70	1.00	0.41	x	(4.18)	0.76
(6) Hatadani	IX	×	○	×	○	ca. 95	<1	<1	ca. 5	0.45	0.88	1.00	0.55	x	(4.45)	1.02
(Mean)	X									0.40	0.92	1.00	0.34	x	1.86	
(*)	XI									0.39	0.85	1.00	0.14	1.87	1.85	

(*) C. Hintze, "Handbuch der Mineralogie," Bd. II, 1115, CCCLVII and CCCLVIII, (1897).

(1) In the analysis of every sample, the ratio of Fe_2O_3/FeO varies considerably, and the reason must be the secondary oxidation of ferrous iron, as often noticed in iron-rich hydrous silicates, such as greenalite[33], stilpnomelane[34], etc., so that in this case, the total iron is regarded as ferrous iron and the molecular ratios are calculated.

(2) A close similarity, therefore, is noticed in the molecular ratio in the analysis of every sample. On close examination, the following facts were brought to light.

(3) The ratio of Al_2O_3/MgO is almost the same in every analysis.

(4) The ratio of FeO/MgO is larger in analyses of samples prepared only when a hand magnet or water washing is used than in those of other samples prepared in different ways.

(5) The ratio of CaO/MgO somewhat varies, and the reason for the variation is not clear, the ratio of CaO/MgO not being proportional to the quantity of augite grains present.

(6) The amount of H_2O (+) is somewhat high in two analyses VIII and IX, Table 9, which must be owing to the content of opal in these two samples, as shown in column [4] in Table 9.

As stated above, it is clear that the part extracted by warm dilute hydrochloric acid shows an almost constant composition corresponding to that of the greenish-coloured mineral now under consideration, whence it follows that the greenish minerals in the foregoing six specimens are of the same species, namely an iron-rich aluminium, calcium, and magnesium hydrous silicate, notwithstanding the moderate variable appearances under the microscope, as stated in the microscopic observations. In the literature on this subject, such hydrous silicates are described as alteration products from augite or amphibole, whereas the iron-rich members are rarely mentioned. Some years ago, Lemberg[35] described an alteration product of augite, showing the chemical compositions as shown in Table 10.

Table 10. Alteration Products from Augite analysed by Lemberg (after Lemberg).

	I	II	Mean	Mol. Ratio	
SiO_2	36.24	37.75	37.00	6161	1.87
Al_2O_3	13.67	12.69	13.18	1293	0.39
Fe_2O_3	23.03	21.69	22.36	—	—
(FeO)	(20.72)	(19.52)	(20.12)	(2801)	(0.85)
CaO	2.79	2.43	2.61	465	0.14
MgO	14.21	12.35	13.28	3294	1.00
H_2O	9.87	12.10	10.99	6106	1.85

From these mean values (Table 10), the molecular ratios are calculated as MgO 1.00, and they upon comparison in Table 9, generally agree with

(33) J. W. Gruner, *Am. Mineral.*, **25**(1938), 172.

(34) C. O. Hutton, *Mineralog. Mag.*, **25**(1938), 172.

(35) Lemberg, *Z. deut. geol. Ges.*, **29**(1877), 495; C. Hintze, "Handbuch der Mineralogie", Bd. II, 1114, Leipzig (1897); C. Doelter, "Handbuch der Mineralchemie," Bd. II, Erster Teil, 572, Leipzig (1917).

Table 11. X-ray Powder Photographs of "Lembergite".

Fig. 38 (9)			Fig. 38 (10)			Fig. 38 (11)			Fig. 38 (12)			Fig. 38 (13)			Fig. 38 (14)			Mean		
I	$2l$ (cm.)	d (A.)	I	$2l$ (cm.)	d (A.)	I	$2l$ (cm.)	d (A.)	I	$2l$ (cm.)	d (A.)	I	$2l$ (cm.)	d (A.)	I	$2l$ (cm.)	d (A.)	I	d (A.)	n
5	2.25	4.58	2	2.30	4.48	7	2.25	4.58	8	2.25	4.58	5	2.25	4.58	3	2.30	4.48	5	4.51	6
5	2.38	4.34				↓			8	2.35	4.39									
						5	2.60	3.97												
												3	2.75	2.76				3	2.76	1
2	2.85	3.63	3	2.85	3.63										2	2.85	3.63	2	3.63	3
						2	2.95	3.51	2	2.95	3.51							2	3.51	2
															2	3.12	3.33	2	3.33	1
			3	3.30	3.15							3	3.23	3.21	2	3.30	3.15	3	3.17	3
						1	3.45	3.02				3	3.45	3.02				2	3.02	2
															10	3.52	2.96	10	2.96	1
2	3.60	2.89	2	3.60	2.89													2	2.89	2
8	4.00	2.61	4	4.00	2.61	5	4.00	2.61	8	4.00	2.61	5	3.90	2.68	5	4.00	2.67	6	2.63	6
8	4.20	2.50	4	4.30	2.44	5	4.40	2.39	8	4.20	2.50	5	4.20	2.50	5	4.20	2.50	6	2.47	6
			1	5.05	2.10							1	5.00	2.12	2	5.00	2.12	1	2.11	3
															2	5.28	2.01	2	2.01	1
															2	5.85	1.83	2	1.83	1
2	6.20	1.74	1	6.15	1.75	2	6.30	1.71	2	6.35	1.70	2	6.15	1.74	2	6.15	1.75	2	1.73	6
2	6.40	1.69	1	6.40	1.69	2	6.65	1.63	2	6.60	1.64	2	6.40	1.69	2	6.70	1.62	2	1.66	6
10	7.15	1.53	10	7.15	1.53	10	7.15	1.53	10	7.15	1.53	10	7.13	1.53	10	7.10	1.54	10	1.53	6
						1	7.65	1.44							3	7.83	1.42	2	1.43	2
2	8.55	1.32	3	8.53	1.32	2	8.55	1.32	2	8.45	1.33	3	8.45	1.33	4	8.50	1.32	3	1.32	6
									2	8.65	1.31									

I: Intensity; d: Measured spacing; $2l$: Distance between two corresponding powder lines measured on the film; n: Number of powder lines measured.

the molecular ratios of the greenish coloured minerals now under consideration. These data strongly suggest that the greenish minerals in the above six specimens are of a species, that is, an alteration product from augite grains, as described by Lemberg[35]. The writer will here refer to the greenish-coloured mineral, mentioned above, as "lembergite".

(VIII) *X-ray Powder Patterns.* The writer took x-ray powder photographs of the powders in which the greenish mineral is concentrated in a practically pure state, as stated in detail in the preceding chapter. A marked similarity will be seen in these photographs as indicated in Fig. 38 (b), (9)–(14), and Table 11. These powders are principally composed of the greenish coloured mineral, as shown in Table 9, [4], then the x-ray powder lines now obtained are mostly derived from the greenish coloured mineral (lembergite).

Although the patterns resemble those of neither chlorites, serpentines, micas nor stilpnomelane, the writer noticed a marked similarity between the x-ray powder photographs of lembergite and those of garnierite, genthite, montmorillonite, and nontronite (Fig. 38).

X-ray Powder Photographs of Garnierite, Genthite, "Lembergite", Montmorillonite, and Nontronite.

Introduction. The writer, upon taking powder photographs of "lembergite," noticed a great similarity between these photographs and those of garnierite, genthite, montmorillonite, and nontronite.

Descriptions of the minerals. (I) *Garnierite*[36]: Garnierite from New Caledonia and the Wakayama mine in Ōita Prefecture, Japan, were used. The former is pale green mass without luster or deep green mass with somewhat vitreous luster, while the latter is dirty-green or pale yellowish-green, soft mass without luster or deep green fragments with somewhat vitreous luster. The analysis of the garnierite from New Caledonia, which is pale green, dull, and massive, is as (dried at 100–110°C.) follows.

SiO_2 46.0, Al_2O_3+Fe_2O_3 2.4, NiO 25.0, MgO 17.6, H_2O (+) 8.5, total 99.5.

Much difficulty was found in securing a sample of garnierite free from impurities from the Wakayama mine, Ōita Prefecture. The analysis of the garnierite, concentrated to the purest degree possible, with some millerite and opal gave:

SiO_2 55.2, Al_2O_3+Fe_2O_3 2.1, CaO tr., NiO 20.1, MgO 5.5, S 2.9, H_2O (+) 5.8, Ignition loss 7.5, total 99.1.

Powder photographs of garnierite have not yet been published. (II) *Genthite*: Genthite from North Carolina was used; it is pale greenish-gray, brittle crust. The chemical analyses of genthite found in the literature of this subject show general similarity to those of garnierite. There is some doubt as to whether these analyses of genthite and garnierite represent those of pure material, if not, the chemically different points

(36) T. Sudo and T. Anzai, *Proc. Imp. Acad.* (*Tokyo*), **18**(1942), 400.

between genthite and garnierite are not clearly established. The writer is of the opinion that genthite differs from garnierite only in the ratio of MgO/NiO, and as will be discussed in detail later, these two species give x-ray powder photographs that are exactly alike, hence it is not necessary to discriminate between these two mineral species.

(III) *Pimelite*: Pimelite from Kosemütz was used. It is a pale greenish-white mass. The writer, upon taking an x-ray powder photograph of it, noticed that the mineral is not pure but that the photograph shows lines of quartz and genthite (or garnierite). As stated above, the x-ray powder photographs of garnierite and genthite are exactly alike, whence the pimelite from Kosemütz is a mixture of quartz and genthite (or garnierite).

(IV) *Montmorillonite*: Montmorillonite from Sibui, Tunetoyomura, Higasi-sirakawa-gun, Hukusima Prefecture, and from Nagatare, Imajuku-mura, Itosima-gun, Hukuoka Prefecture, were used. The former is a pale yellowish-gray, soft mass. Its occurrence has not been described in detail. The analysis gives: SiO_2 48.20, Al_2O_3 13.98, Fe_2O_3 3.84, CaO 2.60, MgO 4.27, H_2O (+) 8.57, H_2O (−) 18.10, total 99.56. The latter is found in pegmatite as a pale pinkish-gray mass.

Montmorillonite is usually found as the main mineral constituent of bentonite clay, and mineralogically, as a species of aluminium hydrous silicate of the metasilicate type. J. W. Gruner[37] gave the general formula of the montmorillonite family,

$$(Al, Fe^{III})_{8+n/3}(Al, Fe^{III})_n Si_{16-n} O_{40}(OH)_8,$$

containing the three species.

Montmorillonite	$n = 0, \quad < 1$
Nontronite	$n = 2\text{-}4$
Beidellite	n lies between the above two limits.

J. W. Gruner noticed that these three mineral species form an isomorphous series. In the classification Table of C. K. Swartz[38], we find the following formulae.

Montmorillonite family

$(Mg, Al, Fe^{III})_{2-3}(Si, Al, Fe^{III})_4 O_{10}(OH)_2 \cdot nH_2O$

Montmorillonite

$(Mg, Al, Fe^{III})_{2-3}(Si_4O_{10})(OH)_2 \cdot 4H_2O$

(Little or no silica replaced by (Al, Fe^{III}))

Nontronite

$(Mg, Al, Fe^{III})_{2-3}(Si, Al, Fe^{III})_4 O_{10}(OH)_2 \cdot nH_2O$

(Up to 1 Si replaced by (Al, Fe^{III}))

H. Berman[39] gave the formula of montmorillonite $(Al, Mg)_8(Si_4O_{10})_3(OH)_{12}$ 12 H_2O with Al/Mg=6:2, which corresponds to that of beidellite $Al_8(Si_4O_{10})_3(OH)_{12}$ 12 H_2O, with part of the Al replaced by Mg.

The analysis of montmorillonite from Sibui, Hukusima Prefecture, gives a formula represented in the general form by J. W. Gruner, as mentioned above.

---

(37) J. W. Gruner, *Am. Mineral.*, **20**(1935), 475.
(38) C. K. Swartz, *Am. Mineral.*, **22**(1937), 1166.
(39) H. Berman, *Am. Mineral.*, **22**(1937), 376.

(V) *Nontronite*: Nontronite from Nontron, Dept. of Dordogne, France, and from Kropfmüle and pinguite (unknown locality) were used. All these are grass-green soft masses. In the earlier days of mineralogy, nontronite was regarded as a species of the kaolinite group[40], but recently J. W. Gruner[41] showed that nontronite and pinguite are members of the montmorillonite group.

Powder photographs. The mineral powders were mixed with collodion and dried, and powder rods obtained, having a mean diameter of about 0.5 mm. A "Fuji Röntgen film", and the camera with a radius of 28.65 mm., determined with a powder photograph of rock salt were used and unfiltered Co radiation was used. The exposures are 2–4 hours. Longer exposures are required for obtaining clear photographs of these minerals than for those of minerals of larger crystals, such as quartz, augite etc. The measured spacings of powder lines are as shown in Tables 11, 12, 13, 14, 15, 16. No corrections were applied to the readings in these tables.

The powder photographs of montmorillonite[42]–[49] and nontronite[50] have already been dealt with by a number of investigators, namely, W. Noll, J. W. Gruner, U. Hoffman, K. Endell, D. Wilm, etc. The measured spacings obtained by some of these investigators are compared with those now obtained, and general agreement is seen. As indicated in the measured spacings obtained by these investigators, in powder photographs of montmorillonite and nontronite, the strongest line giving the measured spacings of 12 to 15 A. are recognized, but since the strongest reflection is obscured by arrangement of the camera used in estimating the relative intensity, the strongest reflection is neglected, and the intensity of the strongest line in the other powder lines is taken as 10 and thus relative intensities of powder lines are estimated.

The relative intensities thus obtained and the measured spacings of powder lines of each powder photograph are shown in Tables 11, 12, 13, 14, 15, 16 and are diagramatically shown in Fig. 38 (a), (b), (c). Next, in the last column of each Table 11, 12, 15, 16, the mean values of the measured spacings and the mean intensities of the corresponding powder lines are described and the mean values of the measured spacings and the mean intensities of the strong lines in each powder photograph of garnierite, genthite (pimelite), "lembergite", montmorillonite and nontronite (pinguite) are compared in Table 17 and diagramatically shown in Fig. 39. In Fig. 39, x-ray powder photographs of chrysotile (Daikwōkō, Kwanden Prefecture, Antō Province, Manchoukuo) and kaolinite (the Zao mine, Miyagi Prefecture) are also compared. From Tables 11, 12, 13, 14, 15, 16, 17 and diagrams (Figs. 38, 39), we have the following facts:

(40) W. Noll, *Chem. Erde*, **5**(1930), 373.
(41) J. W. Gruner, *Am. Mineral.*, **20**(1935), 475.
(42) S. B. Hendricks, and W. H. Ery, *Soil Sci.*, **29**(1930), 457.
(43) P. F. Kerr, *Econ. Geol.*, **26**(1936), 153; *Am. Mineral.*, **17**(1932), 192.
(44) W. P. Kelley, W. H. Dore, and S. M. Brown, *Soil Sci.*, **31**(1931), 25.
(45) U. Hofmann, K. Endell, und D. Wilm, *Z. Krist.*, **86**(1933), 340.
(46) J. D. Laudermilk, and A. O. Woodfold, *Am. Mineral.*, **19**(1934), 260.
(47) J. W. Gruner, *Am. Mineral.*, **20**(1935), 495.
(48) J. W. Gruner, *Am. Mineral.*, **25**(1940), 587.
(49) P. F. Kerr, *Am. Mineral.*, **22**(1937), 534.
(50) J. W. Gruner, *Am. Mineral.*, **20**(1935), 475.

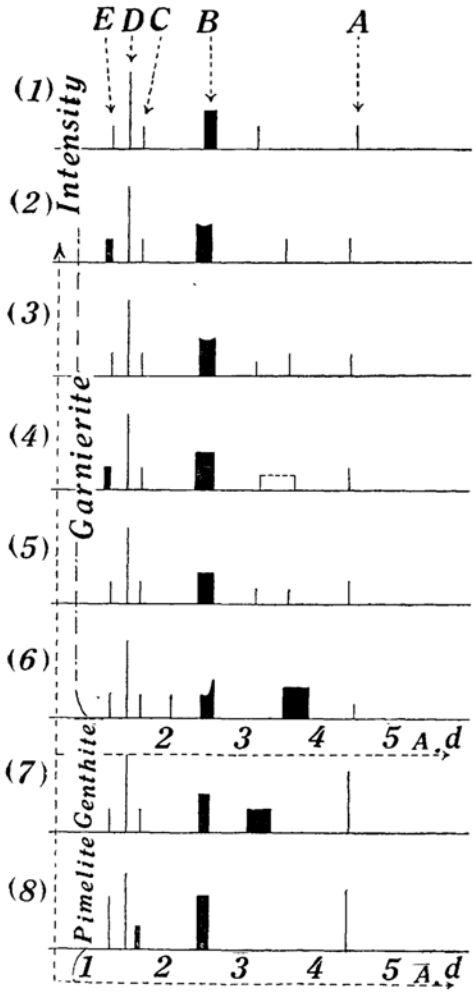

Fig. 38 (a). Diagramatic expression of the spacings (*d* in A.) and relative intensities of the x-ray powder photographs of garnierite, genthite and pimelite. Unfiltered Co radiation. Camera radius 28.65 mm. The lengths of lines in this diagram show roughly the relative intensities of the reflections.

(1) Garnierite (New Caledonia). Pale-green.
(2) Garnierite (New Caledonia). Deep green, with somewhat vitreous lustre.
(3) Garnierite (New Caledonia). Deep green, with somewhat vitreous lustre.
(4) Garnierite (The Wakayama mine, Ōita Prefecture). Deep green, brittle, with somewhat vitreous lustre.
(5) Garnierite (The Wakayama mine, Ōita Prefecture). Dirty-green, brittle.
(6) Garnierite (The Wakayama mine, Ōita Prefecture). Pale yellowish-green, soft, dull.
(7) Genthite (North Carolina).
(8) Pimelite (Genthite + Quartz) (Kosemütz). (Lines due to quartz are eliminated).

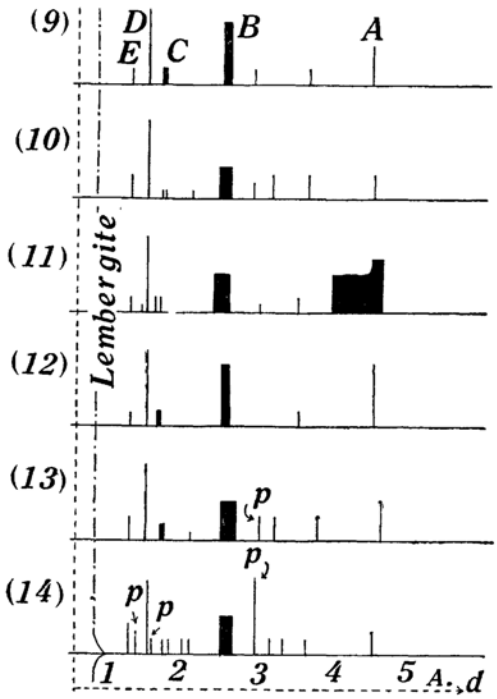

Fig. 38 (b). Diagramatic expression of the spacings (*d* in A.) and relative intensities of the x-ray powder photographs of "lembergite". Unfiltered Co radiation. Camera radius 28.65 mm. The length of lines in this diagram show roughly the relative intensities of the reflections.

p: Lines due to plagioclase.

(9) "Lembergite" (Nasino, Miyagi Prefecture).
(10) "Lembergite" (Kihado, Yamaguti Prefecture).
(11) "Lembergite" (Hatadani, Simane Prefecture).
(12) "Lembergite" (Koganeyama, Simane Prefecture).
(13) "Lembergite" (Kihado, Yamaguti Prefecture). (No. 2).
(14) "Lembergite" (Irisugawa, Gunma Prefecture). (No. 2).

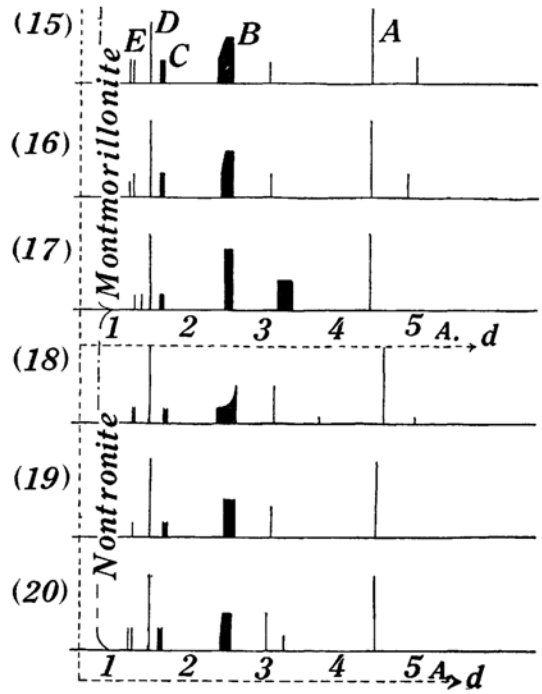

Fig. 38 (c). Diagramatic expression of the spacings (*d* in A.) and relative intensities of the x-ray powder photographs of montmorillonite and nontronite. Unfiltered Co radiation. Camera radius 28.65 mm. The length of lines in this diagram show roughly the relative intensities of the reflections.

(15) Montmorillonite (Sibui, Hukusima Prefecture).
(16) Montmorillonite (Sibui, Hukusima Prefecture) dried at 100°~110°C.
(17) Montmorillonite (Nagatare, Hukuoka Prefecture).
(18) Nontronite (Nontron, Dept. of Dordogne, France).
(19) Nontronite (Kropfmüle). (20) Pinguite (Unknown locality).

(1) Most of the powder lines are broad and diffuse, but a marked similarity is shown in the x-ray powder photographs of these minerals above enumerated. The powder patterns especially of garnierite and genthite agree almost perfectly, showing no differences in the structure of these minerals. The chemical analyses of these two species, garnierite and genthite, as listed in the literature of this subject, are generally similar, and most of them are possibly based on somewhat impure materials, therefore the writer considers that it is not necessary to discriminate these two species.

(2) Each of these x-ray powder photographs is composed of five main powder lines, as indicated in Fig. 39 as A, B, C, D, E.

(3) In each photograph the B line is the broadest. Usually, it is seen as one diffuse line, but in some cases it is separated into two diffuse lines (Fig. 38, (2), (3), (6), (15), (16), (18)). In garnierite, these two powder lines are of almost the same intensity, whereas in montmorillonite and nontronite, the B line is composed of two lines with different intensities.

(4) The C line is seen as a line in the garnierite, genthite and pimelite photographs, but in the other cases, it is seen either as one uniform broad line (Fig. 38, (8), (9), (12), (13), (15), (16), (17)) or two diffuse lines (Fig. 38, (18), (19), (20)) of almost equal intensity, or two sharp lines of equal intensity (Fig. 38, (17), (11), (14)).

(5) The E line is usually seen as a somewhat sharp line, but in other cases it is seen as a uniformly diffused line (Fig. 38, (2), (4) or as two sharp lines of almost equal intensity (Fig. 38, (15), (16), (17), (18), (20)).

(6) The D line is always seen as an intense and relatively sharp line.

(7) The relative intensities of these powder lines are usually the same in every one of these powder photographs. The intensity of line A is almost the same as that of line D in powder photographs of montmorillonite, nontronite, genthite and pimelite, but in the powder photographs of garnierite and genthite, line A is always relatively weaker than line D, and in the powder photograph of "lembergite", the intensity of the A line is medium.

(8) Beside these five main powder lines, some weak ones are seen between A and B lines, some of which are diffuse (Fig. 38, (6), (7), (17)) but the number and measured spacings are variable, even in powder patterns of garnierite.

On close examination, as mentioned above, a marked similarity is noticed in the x-ray powder photographs of these minerals—garnierite, genthite (pimelite), "lembergite", montmorillonite, nontronite (pinguite). Although it is not clear that the powder patterns of "lembergite", now under consideration, are the nearest to whether of the powder photographs of garnierite, genthite, montmorillonite and nontronite, from the above observations, it is believed that powder photographs of "lembergite" are more similar to those of montmorillonite or nontronite than of garnierite or genthite. As stated in detail in the chemical analysis of "lembergite", the mineral is a complex iron-rich hydrous silicate of ferric iron, ferrous iron, aluminium, magnesium, and calcium, therefore "lembergite" may be regarded as a species nearest to nontronite, that is, it probably belongs to the montmorillonite family. The writer gives the following classification.

Garnierite family	Garnierite
	Genthite (pimelite)
	Saponite[51].
Montmorillonite family	Montmorillonite
	Nontronite (pinguite)
	"Lembergite"

(51) It was reported by W. F. Foshag and A. O. Woodfold that x-ray powder patterns of sepiolite and montmorillonite differ. (W. F. Foshag, and A. O. Woodfold, *Am. Mineral.*, **21**(1936), 238). On the other hand, it was described that x-ray powder photographs of saponite and montmorillonite show marked resemblance (C. Palache and H. E. Vassar, *Am. Mineral.*, **10**(1925), 417; P. F. Kerr, *Am. Mineral.*, **22**(1937), 534). From these references and the present writer's study, it is strongly suggested that there is an intimate relation between garnierite and saponite.

It is noticed from earlier descriptions as well as from the writer's observation that these minerals just enumerated all associate intimately with opal or volcanic glass and it is possible that the opal or glass is an important factor for the synthesis of these minerals in nature. The writer also noticed that, in Japan, nontronite or "lembergite" is often the main constituent of some of the diabase or schalstein.

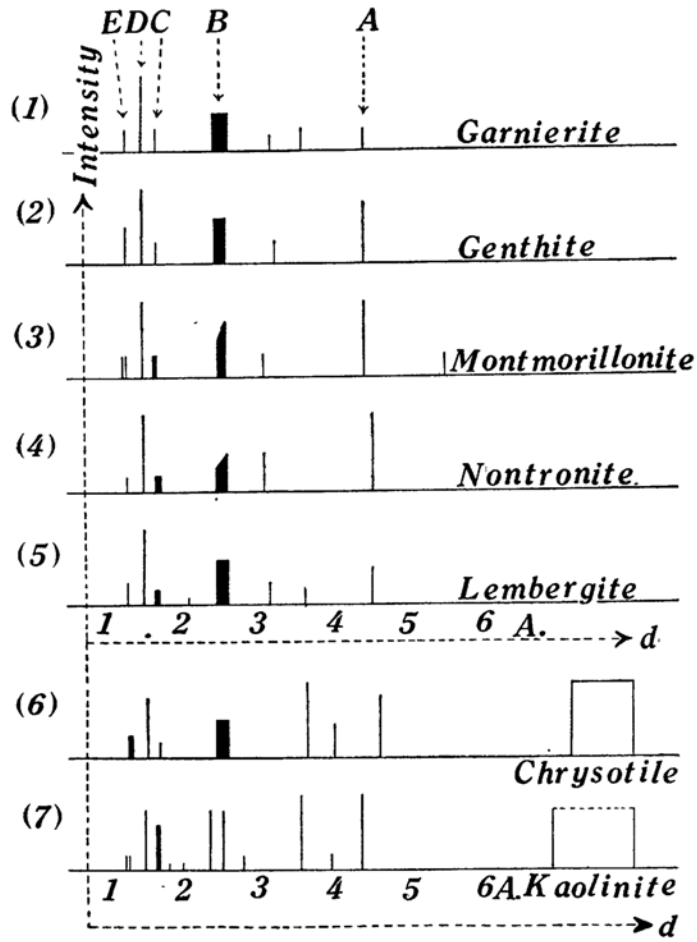

Fig. 39. Diagramatic expression of mean values of interplaner distances—(*d* in A.)—of strong reflections and mean intensities of powder photographs of garnierite, genthite, montmorillonite, and nontronite, compared with the powder photographs of chrysotile (Daikwōkō, Manchoukuo) and kaolinite (the Zao mine, Miyagi Prefecture). Unfiltered Co radiation. Camera radius 28.65 mm. The lengths of lines in this diagram show roughly the intensities of the reflections.

Table 12. X-ray Powder Photographs of Garnierite.

Fig. 38 (1)			Fig. 38 (2)			Fig. 38 (3)			Fig. 38 (4)			Fig. 38 (5)			Fig. 38 (6)			Mean		
I	$2l$ (cm.)	d (A.)	I	$2l$ (cm.)	d (A.)	I	$2l$ (cm.)	d (A.)	I	$2l$ (cm.)	d (A.)	I	$2l$ (cm.)	d (A.)	I	$2l$ (cm.)	d (A.)	I	d (A.)	n
3	2.30	4.48	3	2.35	4.39	3	2.33	4.43	3	2.35	4.39	3	2.35	4.39	2	2.30	4.48	3	4.43	6
															4	2.65	3.90	(4)	(3.90)	(1)
			3	2.90	3.57	3	2.85	3.63	2	2.80	3.70	2	2.85	3.63	4	2.90	3.57	3	3.62	5
3	3.25	3.20				2	3.25	3.20	2	3.20	3.24	2	3.25	3.20				2	3.21	4
5	3.95	2.65	5	4.00	2.61	5	3.95	2.65	5	3.95	2.65	4	3.95	2.65	5	3.95	2.65	5	2.65	6
5	4.20	2.50	5	4.35	2.41	5	4.30	2.44	5	4.40	2.39	4	4.30	2.44	3	4.25	2.47	5	2.44	6
															3	5.00	2.12	3	2.12	1
3	6.35	1.70	3	6.40	1.69	3	6.40	1.69	3	6.40	1.69	3	6.40	1.69	3	6.35	1.70	3	1.69	6
10	7.20	1.52	10	7.20	1.52	10	7.15	1.52	10	7.18	1.52	10	7.15	1.53	10	7.13	1.53	10	1.52	6
3	8.55	1.32	3	8.55	1.32	3	8.55	1.32	3	8.50	1.32	3	8.55	1.32	3	8.55	1.32	3	1.32	6
			3	8.70	1.23				3	8.70	1.23							(3)	(1.23)	(2)

I: Intensity; d: Measured spacing; $2l$: Distance between two corresponding powder lines measured on the film; n: Number of powder lines measured.

Table 13. X-ray Powder Photograph of Genthite (North Carolina) (Fig. 38 (7)).

I	$2l$ (cm.)	d (A.)
8	2.32	4.43
3	3.05	3.40
3	3.35	3.10
5	4.00	2.61
5	4.25	2.47
3	6.40	1.69
10	7.15	1.52
3	8.55	1.32

I: Intensity; d: Measured Spacing; $2l$: Distance between two corresponding powder lines measured on the film.

Table 14. X-ray Powder Photograph of Pimelite (Kosemütz) (Fig. 38 (8)).

	I	$2l$ (cm.)	d (A.)	*	hkl
G	7	2.25	4.58	—	—
G	7	2.45	4.21	—	—
Q	—	2.80	3.70	(3.71)**	—
Q	—	3.10	3.35	3.34	101
G	7	4.00	2.61	—	—
G	7	4.30	2.44	—	—
Q	—	4.60	2.29	2.276	102
Q	—	4.95	2.14	2.123	200
Q	—	5.90	1.82	1.814	112
G	3	6.30	1.71	—	—
G	3	6.50	1.66	—	—
G	10	7.15	1.52	—	—
Q	—	8.07	1.38	1.379	212
G	7	8.67	1.30	—	—

G: Powder lines due to genthite (or garnierite). Q: Powder lines due to quartz. * Calculated values of the spacings of powder lines of quartz. ** After J. Ch. J. Favejee, *Z. Krist.*, **100**(1939), 425. I: Intensity. d: Measured Spacing. $2l$: Distance between two corresponding powder lines measured on the film.

Table 15. X-ray Powder Photographs of Montmorillonite.

Fig. 38 (15)			Fig. 38 (16)			Fig. 38 (17)			Mean		
I	$2l$ (cm.)	d (A.)	I	$2l$ (cm.)	d (A.)	I	$2l$ (cm.)	d (A.)	I	d (A.)	n
3	2.05	5.02	3	2.10	4.91				3	4.97	2
10	2.33	4.43	10	2.23	4.43	10	2.35	4.39	10	4.42	3
						4	3.05	3.40	4	3.40	1
						4	3.25	3.20	4	3.20	1
3	3.35	3.10	3	3.35	3.10				3	3.10	2
6	4.05	2.58	6	4.05	2.58	8	4.05	2.58	7	2.58	3
6	4.15	2.52	6	4.20	2.50	8	4.15	2.52	5	2.47	3
3	4.35	2.41	3	4.25	2.47						
3	6.32	1.71	3	6.35	1.70	2	6.30	1.71	3	1.71	3
3	6.56	1.65	3	6.55	1.65	2	6.60	1.64	3	1.65	3
8	7.33	1.50	8	7.30	1.50	5	7.30	1.50	7	1.50	3
						2	8.05	1.38	2	1.38	1
3	8.75	1.29	3	8.65	1.31				3	1.30	2
						2	8.82	1.28	2	1.28	1
3	9.15	1.25	2	9.10	1.25				3	1.25	2

n: Number of powder lines measured; I: Intensity; d: Measured spacing;
$2l$: Distance between two corresponding powder lines measured on the film.

Table 16. X-ray Powder Photographs of Nontronite.

Fig. 38 (18)			Fig. 38 (19)			Fig. 38 (20)			Mean		
I	$2l$ (cm.)	d (A.)	I	$2l$ (cm.)	d (A.)	I	$2l$ (cm.)	d (A.)	I	d (A.)	n
1	2.05	5.02							1	5.02	1
10	2.25	4.58	10	2.28	4.52	10	2.30	4.48	10	4.53	3
1	2.75	3.76							1	3.76	1
						2	3.15	3.29	2	3.29	1
5	3.30	3.15	4	3.33	3.13	5	3.40	3.06	5	3.11	3
5	3.95	2.65	5	3.96	2.64	5	4.00	2.61	5	2.63	3
↓						5	4.20	2.50			
2	4.35	2.41	5	4.15	2.52	3	4.25	2.47	3	2.47	3
2	6.15	1.75	2	6.15	1.75	3	6.25	1.72	2	1.74	3
2	6.45	1.68	2	6.45	1.68	3	6.50	1.66	2	1.67	3
10	7.15	1.53	10	7.15	1.53	10	7.23	1.52	10	1.53	3
2	8.45	1.33	2	8.55	1.32	3	8.65	1.31	2	1.32	3
2	8.90	1.28	2	8.95	1.27	3	9.03	1.26	2	1.27	3

n: Number of powder lines measured; I: Intensity; d: Measured spacing;
$2l$: Distance between two corresponding powder lines measured on the film.

Table 17. Comparison of Mean Values of Measured Spacings (in A.) and Mean Intensities (I) of Strong Powder Lines in each of the Powder Photographs of Garnierite, Genthite (Pimelite), "Lembergite", Montmorillonite, and Nontronite (Pinguite).

Garnierite			Genthite and Pimelite			"Lembergite"			Montmorillonite			Nontronite and Pinguite		
I	d (A.)	n	I	d (A.)	n	I	d (A.)	n	I	d (A.)	n	I	d (A.)	n
									3	4.97	2			
3	4.43	6	8	4.42	2	5	4.51	6	10	4.42	3	10	4.53	3
3	3.62	5	3	3.40	1	2	3.63	3						
2	3.21	4	3	3.10	1	3	3.17	3	3	3.10	2	5	3.11	3
5	2.65	6	6	2.61	2	6	2.63	6	7	2.58	3	5	2.63	3
5	2.44	6	6	2.47	2	6	2.47	6	5	2.50	3	3	2.47	3
						1	2.11	3						
3	1.69	6	3	1.69	2	2	1.73	6	3	1.71	3	2	1.74	3
						2	1.66	6	3	1.65	3	2	1.67	3
10	1.52	6	10	1.52	2	10	1.53	6	7	1.50	3	10	1.53	3
3	1.32	6	5	1.31	2	3	1.32	6	3	1.30	2	2	1.32	3
									3	1.25	2	2	1.27	3

n: Number of powder lines measured; I: Intensity; d: Measured spacing.

The writer wishes to acknowledge his great indebtedness to Dr. T. Ito, of the Mineralogical Institute at Imperial University, Tokyo, for interest and help shown throughout this work. He also expresses his sincere thanks to Drs. T. Kato, S. Tsuboi, and Y. Otuka, of the Geological Institute at Imperial University, Tokyo, for continuous encouragement and advice and to Dr. E. Minami, of the Chemical Institute at Imperial University, Tokyo, for valuable criticism given for this study. The writer also wishes to take this opportunity to express his thanks to the Council of the Foundation for the Promotion of Scientific and Industrial Researches of Japan for aid granted to defray the expense of printing this paper.

Mineralogical Institute, Imperial University, Tokyo.